Paramagnetic Metal Complexes as Water Proton Relaxation Agents for NMR Imaging: Theory and Design

RANDALL B. LAUFFER

NMR Section, Department of Radiology, Massachusetts General Hospital and Harvard Medical School, Boston, Massachusetts 02114

Received February 26, 1987 (Revised Manuscript Received May 6, 1987)

Contents

Randall B. Lauffer was born in Livermore, CA, in 1957. He received a B.S. in Chemistry from Wake Forest University in 1979 and a Ph.D. from Cornell University in 1983. He was a National Institutes of Health Postdoctoral Fellow from 1984–1986 in the Department of Radiology at Massachusetts General Hospital, Boston, MA, and Harvard Medical School. He is currently director of the NMR Contrast Media Laboratory at Massachusetts General Hospital, a National Institutes of Health New Investigator, and an Assistant Professor at Harvard Medical School in the Radiology Department. His research interests are in the areas of bioinorganic chemistry and NMR, focusing in particular on the interactions between metal complexes and proteins and the development and characterization of metal complexes as diagnostic agents for NMR imaging.

I. Introduction

The development of nuclear magnetic resonance (NMR) imaging techniques as a clinical diagnostic modality has prompted the need for a new class of pharmaceuticals. These drugs would be administered to a patient in order to (1) enhance the image contrast between normal and diseased tissue and/or (2) indicate the status of organ function or blood flow. The image intensity in ^{1}H NMR imaging, largely composed of the NMR signal of water protons, is dependent on nuclear relaxation times. Complexes of paramagnetic transition and lanthanide ions, which can decrease the relaxation times of nearby nuclei via dipolar interactions, have received the most attention as potential contrast agents.

The extension of NMR to in vivo tissue characterization, including both imaging and spectroscopy of metabolites, has brought new chemistry into diagnostic medicine. Paramagnetic contrast agents are an integral part of this trend—they are unique among diagnostic agents. In tissue, these agents are not visualized directly on the NMR image but are detected indirectly by virtue of changes in proton relaxation behavior. In contrast, other diagnostic agents, such as the iodine-containing X-ray contrast agents (which absorb and scatter X-rays) and radiopharmaceuticals, are directly visualized. The lack of ionizing radiation in NMR imaging and in its new contrast media is attractive to physicians (and patients!) as well as basic investigators. Moreover, the development of these agents offers intriguing challenges for investigators in the chemical, physical, and biological sciences. These include the design and synthesis of stable, nontoxic, and tissue-specific metal complexes and the quantitative understanding of their effect on nuclear relaxation behavior in solution and in tissue.

The need for NMR contrast agents and the interesting research problems associated with their development has produced an active research area. Over the past 3 years, roughly 140 reports related to contrast

0009-2665/87/0787-0901$06.50/0

agents have appeared in the literature, and the rate of publication is steadily increasing. Several introductory and review articles are available, mostly in medical journals, covering basic properties and applications of NMR contrast agents.[1-7] The purpose of this review is to communicate the state of the art at this early stage to investigators and to point out interesting and worthy areas deserving their attention. The emphasis here is on the chemical and NMR properties of soluble metal complexes relevant to the design of paramagnetic diagnostic agents. Gadolinium(III), iron(III), and manganese(II) complexes will receive the most attention because of their high magnetic moments and relaxation efficiency. Other substances, such as nitroxide free radicals and suspensions of paramagnetic or ferromagnetic particles, are undergoing more limited examination and will not be discussed.

II. Historical Background

Fundamental investigations leading to the new area of NMR contrast agents are briefly discussed here. Bloch first described the use of a paramagnetic salt, ferric nitrate, to enhance the relaxation rates of water protons.[8] The standard theory relating solvent nuclear relaxation rates in the presence of dissolved paramagnetic substances was developed by Bloembergen, Solomon, and others.[9-12] Eisinger, Shulman, and Blumberg demonstrated that binding of a paramagnetic metal ion to a macromolecule, in their case DNA, enhances the water proton relaxation efficiency via lengthening of the rotational correlation time.[12] This phenomenon, which came to be known as proton relaxation enhancement (PRE), has been utilized extensively to study hydration and structure of metalloenzymes (for reviews, see ref 13-15).

The pioneering 1973 work of Lauterbur[16] toward imaging with NMR was extended to human imaging in 1977.[17] Lauterbur, Mendoca-Dias, and Rudin were first to show the feasibility of paramagnetic agents for tissue discrimination on the basis of differential water proton relaxation times.[18] In their experiments, a salt of manganese(II), a cation known to localize in normal myocardial tissue in preference to infarcted regions, was injected into dogs with an occluded coronary artery. The longitudinal proton relaxation rates ($1/T_1$) of tissue samples correlated with Mn(II) concentration and, thus, normal myocardium could be distinguished from the infarcted zone by relaxation behavior alone. Brady, Goldman, et al. subsequently confirmed the feasibility of paramagnetic agents in imaging studies of excised dog hearts treated in a similar fashion.[19,20] Normal myocardium, containing Mn(II), exhibited greater signal intensity than infarcted regions on NMR images; no contrast was present without Mn(II).

The first human NMR imaging study involving a paramagnetic agent was performed by Young et al.; orally administered ferric chloride was used to enhance the gastrointestinal tract.[21] The diagnostic potential of paramagnetic agents was first demonstrated in patients by Carr et al.[22] Gd(III) diethylenetriaminepentaacetate [$[Gd(DTPA)(H_2O)]^{2-}$] was administered intravenously to patients with cerebral tumors, providing enhancement of the lesion in the region of cerebral capillary breakdown. This is the only agent currently undergoing clinical trials.

III. Dependence of NMR Image Intensity on Tissue Relaxation Times

For a detailed description of NMR imaging techniques, the reader is referred to a number of excellent review articles and monographs.[23] The simplest form of NMR imaging involves the application of a linear magnetic field gradient in addition to the main static field in order to "spatially encode" nuclei in the subject with different resonant frequencies. The free introduction decay signal following a radio frequency pulse is Fourier transformed to yield a one-dimensional projection of signal amplitude along a particular line through the subject. With the aid of algorithms used in X-ray computed tomography (CT) and other imaging applications, a series of such projections can be reconstructed into two-dimensional images of NMR signal intensity.

The dependence of ^1H NMR image intensity on tissue relaxation times (which is the basis of image enhancement using paramagnetic agents) is inherent in the basic principles of pulse NMR.[24] Briefly, the net macroscopic magnetization of proton spins, which is aligned parallel with the applied field along the z axis, is perturbed by application of one or more radio frequency pulses. The component of the magnetization along the z axis "relaxes" back to its equilibrium value with an exponential time constant, T_1, the longitudinal (or spin–lattice) relaxation time. The time dependence of the magnetization perpendicular to the z axis is characterized similarly by T_2, the transverse (or spin–spin) relaxation time, which measures the time for the decay of the transverse magnetization to its equilibrium value of zero. In image data aquisition, the pulses are rapidly repeated for each projection. Tissues with short T_1 values generally yield greater image intensity than those with longer values since the steady-state magnetization along the z axis is greater in the tissue with the fastest relaxation. On the other hand, short T_2 values are always associated with lower signal intensity since this diminishes the net transverse magnetization available for detection.

Under conditions normally employed, the dominant effect of a paramagnetic agent in NMR imaging is to increase the signal intensity of the tissue containing the agent. This is the case because the T_2's of tissues are very short and are not sizably decreased by reasonable (and safe) concentrations of the paramagnetic agent. The greater fractional decrease in T_1 dominates the relaxation effects and generates signal enhancement as described above. The degree of enhancement is dependent on the pulse sequence used for data aquisition. Optimization of pulse sequence parameters for imaging paramagnetic contrast agents has been discussed.[25]

IV. General Requirements for Metal Complexes as NMR Contrast Agents

NMR imaging contrast agents must be biocompatable pharmaceuticals in addition to nuclear relaxation probes. Aside from standard pharmaceutical features such as water solubility and shelf stability, the requirements relevant for metal complex-based agents can be classified into three general categories; a review of the literature pertinent to each category follows this section.

Relaxivity. The efficiency with which the complex enhances the proton relaxation rates of water, referred to as relaxivity, must be sufficient to significantly increase the relaxation rates of the target tissue. The dose of the complex at which such alteration of tissue relaxation rates occurs must of course be nontoxic. As small as 10–20% increases in $1/T_1$ could be detected by NMR imaging.

Specific in Vivo Distribution. Ideally, to be of diagnostic value, the complex should localize for a period of time in a target tissue or tissue compartment in preference to nontarget regions. This is a basic tenet in any agent-based imaging procedure where detection of the agent is usually a simple function of its tissue concentration. For NMR relaxation agents, however, this requirement should be qualified: it is sufficient *only* that the relaxation rates of the target tissue be enhanced in preference to other tissues. This might be accomplished by means other than concentration differences if the complex has a higher relaxivity in the environment of one tissue.

In Vivo Stability, Excretability, and Lack of Toxicity. The acute and chronic toxicity of an intraveneously administered metal complex is related in part to its stability in vivo and its tissue clearance behavior. The transition-metal and lanthanide ions are relatively toxic at doses required for NMR relaxation rate changes; thus, the dissociation of the complex cannot occur to any significant degree. (The toxicity of the free ligand also becomes a factor in the event of dissociation.) Additionally, a diagnostic agent should be excreted within hours of administration.

V. Relaxivity of Metal Complexes

A. Theory and Mechanisms

The NMR relaxation properties of nuclei in the presence of unpaired electron spins and available theoretical approaches for quantitative understanding have been presented.[13,15,26-31] The following summary emphasizes important features relevant to the relaxivity of metal complexes, a subject which has not received sufficient attention, rather than that of aquo ions or protein–metal ion complexes. Our understanding of the structural, dynamic, and magnetic resonance aspects of metal complex relaxivity is still rudimentary in many instances. The existing knowledge base nevertheless provides a crucial starting point for discussing how one might maximize relaxivity in vivo.

1. Contributions to Relaxivity

The addition of a paramagnetic solute causes an increase in the longitudinal and transverse relaxation rates, $1/T_1$ and $1/T_2$, respectively, of solvent nuclei. The diamagnetic and paramagnetic contributions to the relaxation rates of such solutions are additive and given by eq 1, where $(1/T_i)_{obsd}$ is the observed solvent relaxation rate in the presence of a paramagnetic species, $(1/T_i)_d$ is the (diamagnetic) solvent relaxation rate in the absence of a paramagnetic species, and $(1/T_i)_p$ represents the additional paramagnetic contribution. In the absence of solute–solute interactions, the solvent relaxation rates are linearly dependent on the concentration of the paramagnetic species ([M]); *relaxivity*, R_i, is defined as the slope of this dependence in units of M^{-1} s^{-1} or, more commonly, mM^{-1} s^{-1} (eq 2).

$$(1/T_i)_{obsd} = (1/T_i)_d + (1/T_i)_p \quad i = 1, 2 \qquad (1)$$

$$(1/T_i)_{obsd} = (1/T_i)_d + R_i[M] \quad i = 1, 2 \qquad (2)$$

The large and fluctuating local magnetic field in the vicinity of a paramagnetic center provides this additional relaxation pathway for solvent nuclei. Since these fields fall off rapidly with distance, random translational diffusion of solvent molecules and the complex as well as specific chemical interactions that bring the solvent molecules near the metal ion (e.g., within 5 Å) are important in transmitting the paramagnetic effect. Each type of chemical interaction can yield different relaxation efficiencies as governed by the distance and time scale of the interaction; the sum of these contributions and that due to translational diffusion gives the total relaxivity of the paramagnetic species. For the discussion that follows, it is useful to classify the relevant contributions for water proton relaxivity with respect to three distinct types of interactions, as indicated schematically below. In case A, a water molecule binds

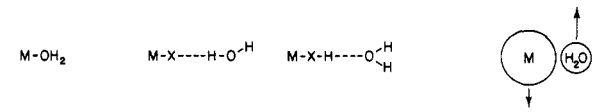

in the primary coordination sphere of the metal ion and exchanges with the bulk solvent. The available theory for solvent relaxation in this case is summarized in the next section. The term "inner-sphere relaxation" is often applied loosely to this type of relaxation mechanism. It should be mentioned, however, that this same theory applies in the case B interaction, i.e., hydrogen-bonded waters in the second coordination sphere, if the lifetime of this interaction is long compared with the time required for the water molecule and the chelate to diffuse past each other. Nevertheless, due to the lack of understanding of second coordination sphere interactions, investigators often do not distinguish between this relaxation mechanism (case B) and that due to translational diffusion of the water molecule past the chelate (case C), referring simply to "outer-sphere relaxation". The total relaxivity of a paramagnetic agent is therefore generally given by eq 3.

$$(1/T_i)_p = (1/T_i)_{inner\ sphere} + (1/T_i)_{outer\ sphere} \quad i = 1, 2 \qquad (3)$$

The following two sections highlight the various quantitative approaches to the understanding of both inner- and outer-sphere relaxivity. The former mechanism has been authoritatively reviewed by Kowalewski et al.[31]; the features pertinent to the relaxivity of metal complexes will be briefly summarized here. To date, the outer-sphere mechanism has not been fully discussed within the context of both experimental observations and theory and is thus covered in somewhat more detail. The effects on longitudinal relaxation behavior are emphasized since these largely control NMR image enhancement.

2. Inner-Sphere Relaxation: Solomon–Bloembergen Equations

The longitudinal relaxation contribution from the inner-sphere mechanism results from a chemical ex-

change of the water molecule between the primary coordination sphere of the paramagnetic metal ion (or any hydration site near the metal) and the bulk solvent as shown in eq 4. Here P_M is the mole fraction of metal

$$\left[\frac{1}{T_1}\right](\text{inner sphere}) = \frac{P_M q}{T_{1M} + \tau_M} \quad (4)$$

ion, q is the number of water molecules bound per metal ion, T_{1M} is the relaxation time of the bound water protons, and τ_M is the residence lifetime of the bound water. The value of T_{1M} is in turn given by the Solomon–Bloembergen equations,[9b,11] which represent the sum of dipolar ("through-space") and scalar, or contact ("through-bonds"), contributions (eq 5), where γ_I is the

$$\frac{1}{T_{1M}} = \frac{2}{15}\frac{\gamma_I^2 g^2 S(S+1)\beta^2}{r^6}\left[\frac{7\tau_c}{(1+\omega_S^2\tau_c^2)} + \frac{3\tau_c}{(1+\omega_I^2\tau_c^2)}\right] + \frac{2}{3}S(S+1)\left(\frac{A}{\hbar}\right)^2\left[\frac{\tau_e}{1+\omega_S^2\tau_e^2}\right] \quad (5)$$

proton gyromagnetic ratio, g is the electronic g-factor, S is the total electron spin of the metal ion, β is the Bohr magneton, r is the proton–metal ion distance, ω_S and ω_I are the electronic and proton Larmor precession frequencies, respectively, and $A/\hbar$ is the electron–nuclear hyperfine coupling constant. The dipolar and scalar relaxation mechanisms are modulated by the correlation times τ_c and τ_e as given by eq 6 and 7, where

$$\frac{1}{\tau_c} = \frac{1}{T_{1e}} + \frac{1}{\tau_M} + \frac{1}{\tau_R} \quad (6)$$

$$\frac{1}{\tau_e} = \frac{1}{T_{1e}} + \frac{1}{\tau_M} \quad (7)$$

T_{1e} is the longitudinal electron spin relaxation time, τ_M is the water residence time as mentioned above, and τ_R is the rotational tumbling time of the entire metal–water unit.

The Solomon–Bloembergen (SB) equations were found to be inadequate in describing the magnetic field dependence of the longitudinal and transverse relaxivities in simple aquo ion solutions such as that of Mn(II). Bloembergen and Morgan developed a theory for the field dependence of T_{1e} that accounted for the discrepancies.[32] For $S > {}^1/_2$ ions, collisions between the complex and solvent molecules (or "wagging" motions of the primary coordination sphere water molecules[33]) are thought to induce distortions from octahedral symmetry that, in turn, lead to transient zero-field splitting (ZFS) of the electronic spin levels. Electronic relaxation occurs as a result of this ZFS modulation, with T_{1e}^{-1} given by eq 8, where the constant B is related to the

$$\frac{1}{T_{1e}} = B\left[\frac{\tau_V}{1+\omega_S^2\tau_V^2} + \frac{4\tau_V}{1+4\omega_S^2\tau_V^2}\right] \quad (8)$$

magnitude of the transient ZFS and τ_V is the correlation time characterizing the flucuations. The inclusion of this expression in the standard SB approach constitutes the Solomon–Bloembergen–Morgan (SBM) equations.

For $S > {}^1/_2$ metal complexes of lower symmetry, a number of problems arise in developing a quantitative description of solvent relaxation. These difficulties have been discussed by several authors, generally in reference to the determination of structural and dynamic parameters in metalloenzyme–water interactions.[15,29–31] The lower symmetry in these molecules results in a static ZFS of the electronic spin levels that demands a more complex form of the spin Hamiltonian describing the electron–nuclear dipolar interaction than that utilized in the standard SB approach. Modified SB equations have been derived for various $S > {}^1/_2$ systems by Koenig et al.[34] and Bertini and co-workers.[35–37] This work has been important in illustrating the effect of ZFS under certain conditions such as the limit of low field. In comparing these modified approaches to experimental data, the Bloembergen–Morgan (BM) equations are employed to account for the field dependence of T_{1e}. Though this theory is not appropriate in the case of static ZFS (see below), it is often used with the justification that this general functional form may approximate the electronic relaxation behavior under any circumstances. Inclusion of the BM equations is especially useful in simulating the competing effects of the multiple parameters involved in relaxivity (see section VC).

The major problems with the standard SB approach or its modified versions involve assumptions concerning electronic relaxation that are often not satisfied in real systems.[31] Rotational modulation of the static ZFS tensor leads to more efficient electronic relaxation than in the absence of ZFS, increasing the importance of T_{1e} in determining τ_c and the net relaxivity. (This decrease in T_{1e} drastically reduces the magnitude of the contact contribution to water proton relaxivity of metal complexes; thus, the dominant dipolar term will be emphasized in all discussions here.) If T_{1e} and τ_R become comparable in magnitude, one of the basic assumptions required by the Redfield theory[38] used in deriving these equations no longer holds. This assumption, referred to as the so-called strong-narrowing condition, demands that the modulation responsible for electronic (or nuclear) relaxation must occur on a much faster time scale that the relaxation time itself; i.e., $\tau_R \ll T_{1e}$. A second problem is that, since electronic relaxation is a function of reorientation, T_{1e} and τ_R are correlated and cannot be treated as independent processes contributing to the overall complexation time.

A more general (and complex) theory has been developed by Lindner,[39] Friedman et al.,[40] and the Stockholm group.[31,41] Relaxivity is predicted to depend on the magnitude of the ZFS, τ_R (and τ_M), and the position of the nucleus relative to the primary axis of the spin tensor. The field dependence of relaxivity calculated from this model is equal to that of the SBM equations only in the limit of low ZFS (ZFS $\ll \omega_S$); with larger ZFS, which is common in $S > {}^1/_2$ ions, the magnitude of the relaxivity decreases, and the functional form, especially that corresponding to the "7-term" of the SB equations, is drastically altered. For $S = 1$ nickel(II) complexes, experimental relaxivities were reported to compare satisfactorily with numerical calculations based on this elaborate theory.[41e]

In comparison with the BM theory of electronic relaxation, in which the electronic structure of the ion is treated as a sphere subject to distortions, the Swedish authors point out that their progress to date has been toward the "nondeformable cigar" model, i.e., anisotropic electronic structure not influenced by additional

ZFS distortions from solvent collisions or ligand vibrations.[31] In all likelihood, both static and transient ZFS interactions modulate electronic relaxation in many systems of interest. A more complete and relevant "deformable cigar" model, in which both mechanisms are operative, is apparently under development.

Kushnir and Navon have reexamined the relaxivity of Mn(II)-substituted metalloenzymes and point out that experimental values measured at high magnetic fields (where the Zeeman energy can be greater than the static ZFS and where T_{1e} can become longer than either τ_R or τ_M) may obviate some of the difficulties discussed above.[42] The measurement of both T_1 and T_2 of ^1H_2O and ^2H_2O at high fields (corresponding to 270–300-MHz proton Larmor frequency) yielded reasonable values for q, τ_M, τ_C, and the outer-sphere contribution when the standard SB equations were utilized. While investigators in NMR contrast agents are interested in relaxivities at intermediate field strengths, where T_{1e} can often play an important role, this high field proton/deuteron method is recommended in order that some of the relevant parameters can be determined. It should be noted, however, that additional spectral density terms may need to be considered for transverse relaxation in the limit of high field.[41b-d] (Also, if τ_R is long, the "Curie spin" mechanism[43] may contribute to the transverse relaxation in addition to the normal dipole–dipole interaction.)

3. Outer-Sphere Relaxation

The outer-sphere contribution to solvent relaxation has received less attention than the inner sphere mechanism. Most studies have focused on aquo metal ions and metal–macromolecule complexes where inner-sphere contributions are quite large. (For aquo ions, this is due to the large number of coordinated water molecules; the macromolecular complexes exhibit long rotational tumbling times and, therefore, high inner-sphere relaxivity when $q \neq 0$). In the design of NMR contrast agents, the use of multidentate ligands to ensure in vivo stability of the complexes reduces the number of coordinated water molecules; the outer-sphere contribution for these low molecular weight complexes thus becomes a significant fraction (if not all) of the total relaxivity.

In contrast to the inner-sphere contribution to relaxivity, which is fundamentally a two-site chemical exchange problem, the so-called outer-sphere component is a more complex problem in solvation dynamics and diffusion. An unambiguous, quantitative understanding of this contribution has not been forthcoming despite its importance in contrast agent design and in understanding second coordination sphere effects in chemical reactions and electron transfer. The subject is treated in some detail here in the hope of stimulating interest in the structural and dynamic aspects of metal complex solvation.

Theory is available to treat the limiting case where no chemical (or electrostatic) interactions occur between water and the metal complex (case C above). The electron–nuclear dipolar interaction in this case is usually modulated by the relative translational diffusion of both species. Several authors have derived expressions to account for this mechanism; these yield qualitatively similiar predictions (with generally broader dispersions of the relaxivity with increasing field compared with SB theory) but differ in how the molecular motion is modeled or whether the effects of off-center electronic distribution or excluded volume are included.[44-47] These approaches have been applied to aqueous solutions of molecular oxygen,[48] methemoglobin,[49] and copper proteins[50] as well as solutions of nitroxide free radicals in water[51,52] and other solvents.[53]

The most general form of the theory for outer-sphere relaxivity incorporates the effects of fluctuations due to electronic relaxation as well as that due to translational diffusion.[44a,46b] The resulting expressions have some similarity with the SB equations, with the longitudinal relaxivity given by eq 9, where C is a numerical

$$\left[\frac{1}{T_1}\right]_{\text{outer sphere}} = \frac{C\pi N_S \gamma_I^2 \gamma_S^2 \hbar^2 S(S+1)}{d^3 \tau_D}[7I(\omega_S, \tau_D, T_{1e}) + 3I(\omega_I, \tau_D, T_{1e})] \quad (9)$$

constant that differs slightly between the different models used to derive the equations,[52] N_S is the number of metal ions per cubic centimeter, d is the distance of closest approach of the solvent molecule to the metal complex, and τ_D, the relative translational diffusion time, is given by eq 10, where D_I and D_S are the diffu-

$$\tau_D = d^2/3(D_I + D_S) \quad (10)$$

sion coefficients of water and the metal complex, respectively. (The other symbols have their usual meaning as described above.) Diffusion coefficients can be estimated if the motion is described by the diffusion of rigid spheres in a medium of viscosity η as shown in eq 11, where a is the molecular radius. The "7-term"

$$D = kT/6\pi a\eta \quad (11)$$

and "3-term" spectral density functions in eq 9 are mathematically complex in both the Pfeifer[44a] and Freed[46b] versions. These two approaches differ in that the latter version includes the finite volume of the paramagnetic molecule. Modifications of these basic equations suitable for low-symmetry electronic environments have not been presented.

The distinction between the hard-sphere diffusion model (case C), to which the Pfeifer equations apply, and the case of transient second coordination sphere solvent interactions (case B) is a difficult one. It is possible that in many instances the diffusion model may account for the relaxivity observed (in terms of its dependence on magnetic field and temperature), although the actual mechanism involves specific solvation interactions. The fact that a complex is soluble in water testifies to such interactions. More direct evidence is available and is briefly reviewed here.

X-ray and neutron diffraction as well as inelastic neutron-scattering studies have detected outer-sphere water molecules in aqueous metal salt solutions.[54,55] Twelve to fifteen waters are located in the second coordination sphere with oxygen atoms approximately 4 Å from the metal ion. The water molecules in the primary coordination sphere exert an orienting effect on the second-sphere waters: the hydrogen atoms of the metal-coordinated waters (which have greater partial positive charge than in bulk water) preferentially

attract the oxygens of those in the second sphere. A similar interaction between the exchange inert ruthenium(III)–hexaamine complex and second coordination sphere water molecules was postulated to account for ^1H and ^{17}O NMR relaxation behavior.[56] Earlier applications of NMR in the detection of outer-sphere interactions involving aquo ions has been reviewed.[57]

Direct evidence of solvation interactions with metal chelate complexes in solution (via diffraction or scattering studies) hss not been presented. Nevertheless, X-ray crystal structures often reveal hydrogen bonding between solvent in the crystal lattice and atoms on the ligand. In solution, various forms of optical spectroscopy commonly detect "solvent effects", and infrared spectroscopy has elucidated specific hydrogen-bonding interactions in solutions (see, for example, ref 58).

NMR studies of paramagnetic chelate solutions clearly reveal preferential orientation of solvent molecules in the second coordination sphere on the basis of selective relaxation or chemical shift effects.[59-64] The quantitative interpretation of the data from these investigations (in terms of the number of second sphere molecules, their residence lifetime and distance to the metal center, and the equilibrium constants for their association with the metal chelate) should be regarded as tentative, particularly in view of the limitations of the Solomon–Bloembergen equations in accounting for relaxation effects from low-symmetry metal centers. However, the data clearly underline the importance of solvation and its *structural* basis. For example, Frankel showed that in methanol solutions of the exchange inert chromium(III)–tris(acetylacetonate) complex the T_2 of the hydroxyl proton was reduced to a much greater extent than that of the methyl protons.[59] Hydrogen bonding to the partial negatively charged acetylacetonate oxygens, observed in infrared studies,[58] places the hydroxyl protons much closer to the paramagnetic metal ion than the methyl group.

In a recent ENDOR study of Gd(III) tris(acetate) in frozen methanol–water solutions, nuclear hyperfine coupling components were detected from methanol protons.[65] The estimated metal–proton distances for the hydroxyl and methyl protons, 3.9 and 3.6–4.2 Å, respectively, are consistent with second coordination sphere methanol bound in a similar fashion as in the $Cr(acac)_3$ solutions. It should be mentioned that Luz and Meiboom provided the first realistic estimates of the distances involved in outer-sphere methanol interactions.[66] Their proton relaxation measurements on cobalt(II) perchlorate/methanol solutions at low temperatures (slow-exchange regime) allowed estimates of 3.9 and 4.6 Å as the closest approach between the metal ion and the hydroxy and methyl protons, respectively.

Of the two types of second coordination sphere interactions shown in case B above, i.e., that involving donation by either the hydrogen or the oxygen of water, the former is expected to yield greater relaxivity since it brings one proton (and possibly both) quite close to the metal ion (2.5–4.0 Å). This type of solvation would appear to be important, especially in multidentate ligand complexes with carboxylate or phenolate donors. The negative charge on the coordinated oxygens, though partially diminished from metal binding, would contribute to sufficient basicity to support one or two hydrogen bonds via its lone-electron pairs. For example, the crystal structure of cobalt(II) *o*-phenylenediaminetetraacetate reveals four hydrogen-bonded waters (two of which are coordinated to a single oxygen) with an average metal–proton separation of 3.4 Å.[67] The remaining available lone pairs on the metal-coordinated oxygens bind sodium cations in the crystal lattice; since these interactions would be absent in dilute solution, a total of eight second coordination sphere water molecules may exist.

The treatment of solvent nuclear relaxation rates when these interactions occur is problematic. As mentioned previously, if the lifetime of the hydrogen-bonded solvent–chelate complex (τ_M') is long relative to τ_D, then the normal Solomon–Bloembergen theory for inner-sphere relaxivity, or modified versions thereof, can be applied. Koenig and co-workers obtained evidence for such long hydrogen bond lifetimes in their nuclear magnetic relaxation dispersion (NMRD) studies (i.e., the measurement of the magnetic field dependence of solvent relaxation rates) of fluoromethemoglobin[49] (the lower limit of τ_M estimated at 0.6 ns), copper(II) and vanadyl (VO^{2+}) transferrin[68] ($\tau_M \sim 5$ ns), and complexes of human serum albumin with nitroxide-labeled fatty acids[52] ($\tau_M \sim 16$ ns). These lower limits of τ_M are long relative to what many believe reasonable lifetimes for such weak interactions. An often cited example supporting short hydrogen bond lifetimes is that the rotational tumbling of water molecules, which involves breaking up to four hydrogen bonds, is characterized by a correlation time in the picosecond range. Hydrogen bonds to the charged oxygens on metal complexes or metalloprotein binding sites (or the partial negative charge on a nitroxide oxygen) may be somewhat stronger and, thus, may exhibit longer lifetimes. Little is known, however, about the solvent dynamics relevant to this case.

Outer-sphere relaxation in the intermediate regime where $\tau_M \sim \tau_D$ may represent a particularly difficult problem in molecular dynamics; no treatments of this case have been presented. NMR relaxation studies of nitroxides in protic organic solvents are nevertheless instructive in this regard.[53] The field dependence of the methyl proton relaxation rates of methanol in the presence of the free radical is well described by the translational diffusion model; the relaxation rates of the hydroxyl proton, on the other hand, are much greater and seem to be modulated by the rotational motion of a solvent–nitroxide complex involving a hydrogen bond to the nitroxide oxygen. The lifetime of the interaction with methanol was estimated as 10 ps. (Interestingly, the lifetime of the isopropanol complex appeared to be 600 ps!) Translational and rotational mechanisms are most likely operative (and additive) in the relaxivity of both types of protons, but the proton–electron distance in the complex determines the relative contributions.

B. Experimental Results

Water proton relaxation studies of metal chelate compounds have begun to appear relatively recently, linked with the growing availability of pulse NMR spectrometers. Table I is an extensive compilation of measured longitudinal relaxivities (R_1) for aquo ions and low molecular weight metal complexes. This listing should suffice to catalogue relaxivities to date for investigators involved in NMR contrast agent design or

physicochemical aspects of metal chelates and solvation. The field dependence of R_1 obviously presents a problem in a display such as this. Values measured at field strengths in the range of clinical ^{1}H NMR imaging devices (1–80 MHz) are emphasized with very low field values (~0.02 MHz) included when available to show the limiting R_1 as H_0 goes to zero. The reader is referred to the recent work of Koenig, Brown, and co-workers for the full field dependence or NMRD profiles (0.01–50 MHz) of a number of complexes.[69-73]

Also listed in Table I are the number of coordinated water molecules (q) for each complex. The values given are in the best understanding of the author after reviewing available X-ray crystal structures or chemical properties. No value is given if conflicting reports exist or if there is evidence that two or more chemical species are present in solution.

1. Outer-Sphere Relaxivities (q = 0)

Examination of the R_1 values for complexes with q = 0 reveals that outer-sphere relaxivity is indeed appreciable. A rule of thumb is that, for a particular metal ion, this contribution is comparable to the inner-sphere contribution of q = 1 in a complex with similar donor atoms and/or symmetry. It is clear that in no case can the outer-sphere component be ignored in metal complexes.

For metal ions with relatively long T_{1e}'s, the magnitude of the outer-sphere relaxivity scales roughly with the square of the effective magnetic moment [or $S(S + 1)$ value] of the metal ion. If the outer-sphere contribution for chromium(III) complexes ($S = {}^3/_2$) is taken as 0.5 mM^{-1} s^{-1} (20 MHz, 37 °C), the measured relaxivities for coordinatively saturated complexes of Gd(III) ($S = {}^7/_2$; R_1 = 2.0–2.6 mM^{-1} s^{-1}), Mn(II) ($S = {}^5/_2$; R_1 = 1.1–1.3 mM^{-1} s^{-1}), and iron(III) ($S = {}^5/_2$; R_1 = 0.73–0.95 mM^{-1} s^{-1}) compare well with the predicted values (2.1 mM^{-1} s^{-1} for $S = {}^7/_2$ and 1.13 mM^{-1} s^{-1} for $S = {}^5/_2$).

A dependence on the T_{1e} of the metal ion can also be seen in the outer-sphere data. For example, the lower R_1's for iron(III) complexes compared with analogous manganese(II) compounds reflect the shorter T_{1e}'s in the former case. More drastic differences are found in the lanthanide(III)–tris(dipicolinate) complexes. The Gd(III) complex, where T_{1e} is probably on the order of 0.1–1 ns, has an outer-sphere R_1 of 2.6 mM^{-1} s^{-1}, whereas the analogous terbium(III) and dysprosium(III) complexes exhibit R_1's more than one order of magnitude smaller (0.05–0.1 mM^{-1} s^{-1}) due to their very short T_{1e}'s (0.1–1 ps).

As mentioned previously, the actual mechanism and quantitative understanding of the outer-sphere relaxivity of metal complexes have not been satisfactorily established. Knowledge of whether the mechanism involves second coordination sphere interactions, translational diffusion, or both is important in (1) learning how to optimize R_1's and (2) estimating outer-sphere contributions to better characterize inner-sphere relaxivities.

Oakes and Smith suggested that the outer-sphere R_1 of the Mn(II) complexes of EDTA and EGTA is due to eight second coordination sphere waters hydrogen bonded to the four coordinated carboxylate oxygens.[74] Assuming a correlation time of 8.9×10^{-11} s, they calculate a proton–manganese distance of 3.7 Å from the R_1 of $Mn(EGTA)^{2-}$. Despite the fact that the authors use the Solomon–Bloembergen relationships for this estimate, which may not be strictly applicable to the case of transient solvation, the values seem reasonable, and the model of second coordination sphere relaxivity appears plausible.

These authors use the R_1 of $Mn(EGTA)^{2-}$ to estimate the outer-sphere contribution in $Mn(EDTA)(H_2O)^{2-}$.[74] This procedure is commonly criticized in that difference in ligand field, ZFS, T_{1e}, the number of hydrogen-bonding sites, and other chemical features of the two complexes can lead to erroneous estimates.

The use of the Pfeifer equations to calculate outer-sphere relaxivities based on the translational diffusion model underestimates the observed relaxivities. If reasonable assumptions are made regarding the diffusion coefficients of water and the complex as well as the distance of closest approach (in a hard-sphere model), the calculated values can be up to five times smaller that what is observed. For example, Bloch and Navon[75] estimated an outer-sphere R_1 of $Fe(EDTA)(H_2O)^-$ of 0.175–0.27 mM^{-1} s^{-1} (40 MHz, 20 °C), whereas the R_1 of $Fe(DTPA)^{2-}$, a structurally similar but coordinatively saturated complex, is 0.83 mM^{-1} s^{-1} (60 MHz, 20 °C).[76] This underestimation may have led to the unreasonably short metal–proton distance calculated for the former complex; the authors mention second coordination sphere interactions not taken into account by the Pfeifer treatment as a possible source of the additional relaxivity that led to the anomalous r value.

Koenig, Brown, and co-workers recently reported the NMRD profiles for several coordinatively saturated Mn(II) complexes, noting that the data were well described by the Pfeifer equations. In one report, the NMRD profile of $Mn(NOTA)^-$ yields values of 3.1 Å for d, the closest approach distance, 14 ps for τ_D, the translational diffusion correlation time, and ~50 ps for T_{1e}.[72] The data for three complexes were collectively fit in a different paper without the inclusion of T_{1e}; d was found to be 3.5 Å and τ_D was 44 ps.[69] Since the dispersion curves are rather featureless, it is possible to obtain adequate fits with different sets of parameters or even with a different theoretical model. It is interesting that the d values obtained are much shorter than the closest approach distance estimated from the molecular dimensions of similar complexes.[75,77] This suggests that either (1) the solvent molecules are highly oriented in their diffusion path past the complex, or (2) true second coordination sphere adducts are present and the relaxivity is fortuitously well described by the Pfeifer treatment because of the transient nature of the interaction ($\tau_M' \sim \tau_D$).

Clearly, a better understanding of the mechanism and quantitative modeling of outer-sphere relaxation is needed. It would be desirable to measure relaxivities over a wider range of field strengths, perhaps 0.01 or 0.1 MHz to 300–500 MHz; current field cycling methods achieve only 50 MHz. The study of relaxivities in methanol or other protic organic solvents could also help elucidate structure in the second coordination sphere, as previously discussed in reference to nitroxide free radicals. The dependence of outer-sphere relaxivity on the number of metal-coordinated hydrogen-bonding sites, which one envisions is a basic tenet of the second coordination sphere model, has not been investigated.

TABLE I. Longitudinal Relaxivities (R_1) and the Number of Coordinated Water Molecules (q) for Low Molecular Weight Complexes

complex	q^a	R_1, mM^{-1} s^{-1}	freq, MHz	temp, °C	ref	complex	q^a	R_1, mM^{-1} s^{-1}	freq, MHz	temp, °C	ref
						Gd(III)					
aquo ion	8, 9	34.3	0.02	5	*b*			4.7	20	25	69
		26.5	0.02	25	*b*			3.4	20	37	7, 89
		22	0.02	35	69	DTPA	1	7.7	0.02	25	69
		21.4	10	5	*b*			6.7	0.02	35	70
		16.1	10	25	*b*			6.2	6.25	23	129
		9.1	20	35	69			5.6	10	23	125
		9.1	90	37	*c*			4.8	20	25	69
EDTA	2, 3	25	0.02	5	72			4.1	20	35	70
		15	0.02	25	69			3.7	20	37	7, 89
		12	0.02	35	70			4.5	20	37	118
		12	20	5	72	tris(dipic)	0	4.2	0.02	37	*d*
		7.6	20	25	69			2.6	20	37	*d*
		6.6	20	35	70	EGTA	u	3.4	20	30	*e*
		5.4	20	37	7, 89	TETA	0	3.3	0.02	37	69
		6.9	20	37	118			5.2	10	23	125
		4.6	90	37	*c*			2.1	20	37	69
DOTA	1	11.3	0.02	25	69			2.1	20	37	7, 89
		7.2	10	23	125	TTHA	0	2.0	20	37	7
						Mn(II)					
aquo ion	6	44	0.02	35	69	DOTA	u (0?)	2.6	0.01	25	69
		15.5	6.25	23	129			1.7	10	25	69
		7.4	20	35	69			1.1	20	37	7, 89
		8.0	20	37	*f*	DTPA	0	3.4	0.02	5	72
		6.3	40	rt	*g*			2.4	0.02	25	69
		7.4	60	20	74			2.1	0.02	35	70
		5.2	90	37	*c*			2.2	20	5	72
NTA	2	4.4	40	rt	*g*			1.5	20	25	69
EDTA	1	5.6	0.02	25	69			1.3	20	35	70
		4.8	0.02	35	70			1.1	20	37	7, 89
		3.3	20	25	69			1.6	60	20	76
		2.9	20	35	70	EGTA	0	1.7	60	20	85
		2.0	20	37	7, 89	NOTA	0	3.3	0.02	5	72
		3.3	40	rt	*g*			2.3	0.02	25	69
		3.3	60	20	74			2.3	20	5	72
		2.1	90	37	*c*			1.6	20	25	69
						Mn(III)					
acetate, tris	u	4.0	20	37	*f*			19	20	5	73
TPPS	2	6.9	0.02	5	73			15	20	20	73
		7.3	0.02	20	73			12	20	35	73
		7.8	0.02	35	73	[14]aneN$_4$	2	3.08	6.25	23	129
						Fe(III)					
aquo ion	6	17	0.02	35	69			2.55	22	20	75
		8.0	20	35	69			2.23	60	20	75
		11.1	60	20	85			1.7	60	20	85
		5.0	90	37	*c*			1.4	90	37	*c*
TPPS	1	12	0.02	5	73	EHPG	0	0.95	20	37	127
		11	0.02	20	73	5-Me-EHPG	0	1.06	20	37	128
		9.4	0.02	35	73	5-Cl-EHPG	0	0.96	20	37	128
		5.8	20	5	73	5-Br-EHPG	0	0.96	20	37	128
		5.3	20	20	73	EGTA	u (0?)	0.5	60	20	85
		4.8	20	35	73	DOTA	u (0?)	0.4	20	37	7, 89
		3.9	20	37	*f*	DTPA	0	0.92	0.02	37	69
EDTA	1	2.5	0.02	37	69			0.72	20	37	69
		1.8	20	37	69			0.73	20	37	127
		1.9	20	37	*f*			0.7	20	37	7, 89
		1.6	20	37	7, 89			0.83	60	20	76
						Cr(III)					
aquo ion	6	23.5	0.02	35	69	hexafluoro	0	1.3	28.9	25	*h*
		5.8	20	35	69	hexaamine	0	0.59	28.9	25	*h*
		7.2	28.9	25	*h*	tris(oxalate)	0	0.57	28.9	25	*h*
EDTA	1	1.1	2.5	rt	*i*	hexacyano	0	0.48	28.9	25	*h*
		0.2	20	37	7, 89	tris(en)	0	0.50	28.9	25	*h*
						Cu(II)					
aquo ion	6	1.6	0.02	35	69	Me$_4$[14]aneN$_4$	1	0.22	6.25	23	129
		1.47	6.25	23	129	TPPS	u	0.14	20	37	*f*
		0.81	20	35	69	EDTA	u	0.21	60	20	85
		0.84	20	37	*f*	DTPA	0	0.12	60	20	76
		0.74	60	20	85	EGTA	u	0.15	60	20	85
[14]aneN$_4$	1	0.23	6.25	23	129						

TABLE I (Continued)

complex	q^a	R_1, mM^{-1} s^{-1}	freq, MHz	temp, °C	ref	complex	q^a	R_1, mM^{-1} s^{-1}	freq, MHz	temp, °C	ref
					Co(II)						
aquo ion	6	0.15	60	20	85	EGTA	u	0.065	60	20	85
EDTA	u	0.081	60	20	85	DTPA	u	0.054	60	20	76
					Ni(II)						
aquo ion	6	0.78	60	20	85	EGTA	u	0.074	60	20	85
EDTA	u	0.11	60	20	85	DTPA	u	0.106	60	20	85
					Dy(III)						
aquo ion	8, 9	0.56	20	39	78	EDTA	2, 3	0.17	20	39	78
dipic	6	0.38	20	39	78	DTPA	1 (?)	0.096	20	39	78
bis(dipic)	3	0.24	20	39	78	tris(dipic)	0	0.11	20	39	77
					Tb(III)						
aquo ion	8, 9	0.32	20	39	78	EDTA	2, 3	0.14	20	39	78
dipic	8	0.25	20	39	78	DTPA	1 (?)	0.083	20	39	78
bis(dipic)	3	0.16	20	39	78	tris(dipic)	0	0.058	20	39	77
					Nd(III)						
aquo ion	8, 9	0.021	20	39	78	EDTA	2, 3	0.012	20	39	78
dipic	6	0.018	20	39	78	DTPA	1	0.009	20	39	78
bis(dipic)	3	0.014	20	39	78	tris(dipic)	0	0.003	20	39	77

[a] Value given if known from X-ray crystal structure or deduced from analogous complexes; u = unknown. [b] Koenig, S. H.; Epstein, M. *J. Chem. Phys.* **1975**, *63*, 2279. [c] Brown, M. A.; Johnson, G. A. *Med. Phys.* **1984**, *11*, 67. [d] Conti, S.; Lauffer, R. B., unpublished results. [e] Dwek, R. A.; Richards, R. E.; Morallee, K. G.; et al. *Eur. J. Biochem.* **1971**, *21*, 204. [f] Chen, C.; Cohen, J. S.; Myers, C. E.; et al. *FEBS Lett.* **1984**, *168*, 70. [g] King, J.; Davidson, N. *J. Chem. Phys.* **1958**, *29*, 787. [h] Morgan, L. O.; Nolle, A. W.; Hull, R. L.; et al. *J. Chem. Phys.* **1956**, *25*, 206. [i] Runge, V. M.; Foster, M. A.; Clanton, J. A.; et al. *Radiology (Easton, Pa)* **1984**, *152*, 123.

The study of a series of complexes where, for example, the number of carboxylates is systematically varied without greatly altering other properties would be helpful.

2. Low Molecular Weight Metal Complexes with $q \neq 0$

While the reactivity of the symmetrical paramagnetic aquo ions has been quantitatively understood for some time, that of metal chelate compounds has eluded precise and unambigous characterization. This is no doubt linked to the problem of separating inner- and outer-sphere contributions properly and to the limitations of Solomon–Bloembergen theory for low-symmetry metal ion environments. The available studies, which should be read critically with reference to quantitative deductions, nevertheless are important starting points for the design of NMR contrast agents and provide interesting perspectives on metal complex hydration.

The complexation of an aquo ion with a multidentate ligand displaces a number of coordinated water molecules and generally reduces R_1. This was nicely demonstrated by Alsaadi et al. in a proton relaxation study of lanthanide(III) complexes.[77,78] For a given metal ion, a continuous decrease in R_1 is observed in complexes of ligands with increasing denticity. The results for most of the metal ions were interpreted on the basis of a total coordination number of nine, and the decrease in q is equal to the number of donor atoms in the ligand(s).

The DTPA, DOTA, and TETA complexes of Gd(III) are of considerable interest in the design of NMR contrast agents. All three ligands are potentially octadentate. The relaxivities of the DTPA and DOTA complexes are similar and consistent with $q = 1$ in solution; this agrees with the crystal strucures of the neodymium(III)[79] and europium(III)[80] analogues, respectively. The larger macrocyclic ring size for TETA, however, draws the ion closer to the plane of nitrogen donors, resulting in crowding of the carboxylates and loss of a potential open coordination site; the terbium(III) complex has no coordinated water in the solid state.[81] The lower relaxivity for the Gd(III)–TETA complex compares well with other coordinatively saturated complexes ($q = 0$). (This, however, disagrees with solution-state studies of the analogous Eu(III) complex by the luminescence method, where q was found to be 0.6.[77])

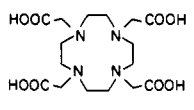

DOTA

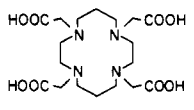

TETA

The q for the EDTA complex of Gd(III) is not well defined. Geier et al. have reported temperature-dependent electronic absorption spectra for the EDTA complexes of samarium(III), europium(III), and Gd(III).[83] Their results were interpreted on the basis of a decrease in q (most likely by 1 unit) at the higher temperatures. Judging from available solid-state X-ray data,[84] the equilibrium is most likely between $q = 3$ at low temperatures and $q = 2$ at higher temperatures.

Oakes and Smith proposed a different type of solution-state equilibrium in their proton relaxation studies of transition-state–EDTA complexes.[85] Assuming that the outer-sphere relaxivities are well approximated by the corresponding EGTA complexes, the authors calculate q values of 0.19, 0.33, and 0.38 for the cobalt(II), nickel(II), and copper(II) complexes, respectively, using the Solomon–Bloembergen equations. A dynamic equilibrium between fully hexadentate (outer-sphere) and pentadentate ($q = 1$) complexes was proposed. The results for the Mn(II) and Fe(III) analogues, on the other hand, were consistent with $q = 1$ as found in the solid state.

A more complete study of $[Fe(EDTA)(H_2O)]^-$ was performed by Bloch and Navon employing ^1H, ^2H, and

TABLE II. Selected Longitudinal Relaxivities (R_1) for Protein–Metal Ion Complexes and for Bovine Serum Albumin (BSA) Covalently Labeled with Metal Chelates

complex	R_1,[a] M^{-1} s^{-1}	freq, MHz	temp, °C	ref
	Gd(III)			
glutamine synthetase	148	22.5	25	*b*
immunoglobulin	112	20	19	*c*
concanavalin A	60	20	25	70
BSA	72	24.3	30	*d*
(BSA)(GdEDTA)$_n$[e]	36	20	37	88
EDTA (free)	6.6	20	35	70
(BSA)(GdDTPA)$_n$	19	20	37	88
DTPA (free)	4.1	20	35	70
	Mn(II)			
pyruvate kinase	275	20	25	28
concanavalin A	96	20	25	70
carboxypeptidase	43	20	25	28
(BSA)(MnEDTA)$_n$	26	20	37	88
EDTA (free)	2.9	20	35	70
(BSA)(MnDTPA)$_n$	3.4	20	37	88
DTPA (free)	1.3	20	35	70
	Fe(III)			
fluoromethemoglobulin	7.3	20	6	28
methemoglobin	1.4	20	6	28
transferrin	2.6	20	38	28
	Cr(III)			
transferrin	2.0	20	38	28

[a] R_1/metal ion. [b] Eads, C. D.; Mulqueen, P.; Horrocks, W. D.; Villafranca, J. J. *Biochemistry* **1985**, *24*, 1221. [c] Burton, D. R.; Forsen, S.; Karlstrom, G.; et al. *Eur. J. Biochem.* **1976**, *71*, 519. [d] Reuben, J. *Biochemistry* **1971**, *15*, 2834. [e] n = 3–10 (average number of chelates/protein molecule).

^{17}O relaxation time measurements.[75] The residence time, τ_M, of the single water was found to be 1.3 μs at 20 °C. As discussed by the authors, the values of other parameters obtained are subject to the inappropriateness of the Solomon–Bloembergen and Bloembergen–Morgan equations and their outer-sphere relaxivity estimation.

Mn(III)–metalloporphyrin complexes have anomalously high relaxivities. This is discussed in section VC1.

3. Protein-Bound Metal Ions and Chelates

Table II is a miscellaneous listing of R_1's measured for metal ions or chelates bound to protein molecules. Values measured at ~20 MHz are emphasized for comparison purposes. The enhancement in relaxivity observed upon attachment of a metal ion to a macromolecule, the PRE effect, can be as high as two orders of magnitude. The reader is referred to other sources for discussions of metalloprotein relaxivity.[13-15,30,86] The purpose here is simply to reiterate the high R_1 values achieved in slowly rotating systems. While the q values for most of the highly efficient species may be higher than that available in stable metal complexes suitable for in vivo applications, the mere existence of these systems is important in stimulating ideas for relaxivity optimization (see section IIIC).

The PRE effect is also operative when intact chelates are covalently attached to protein amino acid residues. Lauffer et al. attached EDTA and DTPA to amino groups on bovine serum albumin (BSA) and bovine immunoglobulins using cyclic anhydride forms of the ligands.[87,88] The structure of the bound ligands, shown in Figure 1, most likely involves an amide linkage between a ligand carboxylate and the lysine or terminal amino groups. Metal ions can be titrated selectively into the chelating sites on the proteins. The 20-MHz R_1's for the Gd(III) and Mn(II) chelates attached to BSA are shown in Table II along with the values for the free chelates from Table I. The relaxivities increase by a factor of two to ten upon attachment, depending on the chelate.

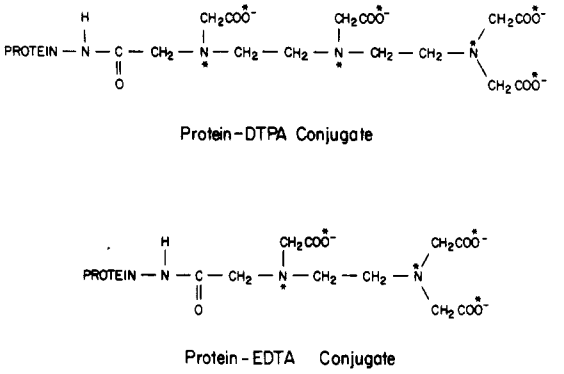

Figure 1. Anticipated structure of the DTPA and EDTA ligands when covalently attached to protein amino groups. Heteroatoms most likely involved in Mn(II) or Gd(III) binding are denoted with asterisks. Reprinted with permission from ref 88. Copyright 1986 Pergamon.

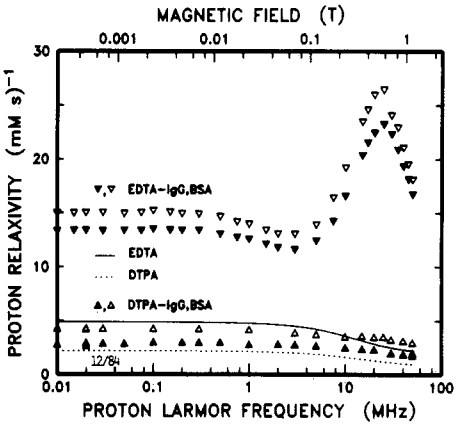

Figure 2. NMRD profiles of Mn(II) chelates covalently attached to protein amino groups. Data are shown for MnEDTA attached to bovine immunoglobulins (IgG, ▼) and bovine serum albumin (BSA, ▽) and the corresponding MnDTPA conjugates (▲, △). The solid and dashed curves in the lower portion of the figure indicate data for the free chelates $Mn(EDTA)^{2-}$ and $Mn(DTPA)^{3-}$, respectively. Reprinted with permission from ref 88. Copyright 1986 Pergamon.

The magnetic field dependence of the relaxivities of the conjugates are more informative.[88] Figures 2 and 3 display the complete NMRD profiles of the free and bound Mn(II) and Gd(III) chelates. Binding is generally accompanied by an increase in the amplitudes of the curves and a change in their functional form, resembling that observed in slowly rotating metalloenzyme systems. This implies that, despite the potentially flexible linkage to the protein, the chelates appear to be fairly immobilized. (The effect of rotational properties on relaxivity is discussed further in section VC3). The magnitudes of the relaxivities most likely relate to the average number of coordinated waters in each case, which is greater for the EDTA conjugates than the DTPA conjugates. It is noteworthy that the low amplitude and featureless NMRD profiles of the Mn–DTPA conjugates, not unlike that of the freely

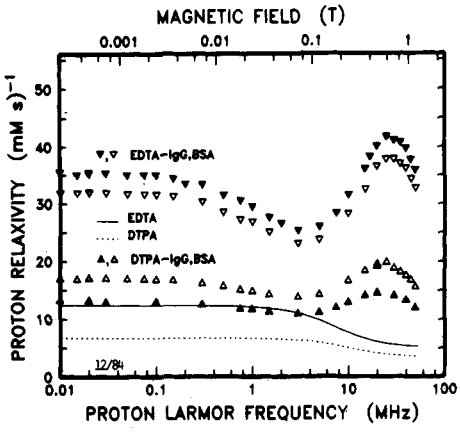

Figure 3. NMRD profiles of Gd(III) chelates covalently attached to protein amino groups. Data are shown for GdEDTA attached to bovine immunoglobulins (IgG, ▼) and bovine serum albumin (BSA, ▽) and the corresponding GdDTPA conjugates (▲, △). The solid and dashed curves in the lower portion of the figure indicate data for the free chelates $Gd(EDTA)^-$ and $Gd(DTPA)^{2-}$, respectively. Reprinted with permission from ref 88. Copyright 1986 Pergamon.

rotating complex, is consistent with outer-sphere relaxation as expected due to the high denticity of the protein-bound ligand.

4. Relaxivity in Tissue

The most important effect of a paramagnetic agent is to enhance the longitudinal relaxation rate of the water protons in tissue. The efficiency by which a complex influences tissue relaxation rates is dependent on two factors: (1) The chemical environment(s) encountered by the complex in vivo. By far the greatest effect is exerted by binding of the agent to macromolecular structures, which can potentially cause significant relaxivity enhancement. (2) Compartmentalization of the complex in tissue. Generally, tissue water is compartmentalized into intravascular, interstitial (fluid space between cells and capillaries), and intracellular space comprising roughly 5, 15, and 80% of the total water, respectively. Cellular organelles further subdivide the intracellular component. If water exchange between any of these compartments is slow relative to the relaxation rate in the compartment with the longest T_1, multiexponential longitudinal relaxation may result. This can decrease the effective tissue relaxivity of an agent because all of the tissue water is not encountering the paramagnetic center.

Estimates of tissue relaxivities of metal complexes require the measurements of excised tissue T_1's from two groups of animals: those receiving the agent and a control group. The tissue concentration of the complex should be determined by analysis of the tissue for metal content or by use of a suitable radioactive tracer. The largest source of error in these determinations is the animal-to-animal variation in baseline relaxation rates.

For low molecular weight hydrophilic metal complexes, the available data show clearly that the relaxivity in blood and soft tissue is within experimental error of that in aqueous solution; this has been shown, for example, for $[Gd(DTPA)(H_2O)]^{2-}$ and $[Gd(DOTA)(H_2O)]^-$ by Tweedle et al.[7,89] This suggests that no binding interactions between the chelate and proteins or membrane structures are taking place. The early use of $Co(EDTA)^{2-}$ as an extracellular marker suggests that the distribution of these Gd(III) complexes is the same.[90] The hydrophilic nature of the complexes as well as their extracellular localization (where protein concentrations are lower relative to intracellular environments) apparently results in unhindered rotational mobility.

Koenig et al. measured NMRD profiles for blood containing $[Gd(DTPA)(H_2O)]^{2-}$.[27-29,91] The single exponential decay of the longitudinal relaxation in these samples indicate that water exchange between erythrocytes and plasma must be fast relative to the relaxation rates. It is interesting that the NMRD difference curves obtained after subtracting out the diamagnetic contribution to the observed rates were identical in amplitude and functional form with that of the complex in aqueous solution.

Compartmentalization effects have been noted for the kidney by Koenig, Wolf, and co-workers in another study of $[Gd(DTPA)(H_2O)]^{2-}$.[27-29,92] Longitudinal relaxation in the renal medulla was found to be biexponential in the presence of the paramagnetic agent, resulting from concentration of the agent in the collecting tubules.

The most prominent evidence for a paramagnetic agent binding in vivo and generating greater relaxivity is that of the Mn(II) ion. Though not relevant as a contrast agent due to its toxicity, Mn(II) has both a historical and instructive importance. Lauterbur, Mendonca-Dias, and Rudin, in their landmark 1978 paper, noted an approximately 50% increase in relaxivity for Mn(II) in heart tissue at 4 MHz.[18] Kang and Gore measured enhancement factors (relative to the aquo ion in aqueous solution) of four to six at 20 MHz for Mn(II) in heart, liver, spleen, and kidney.[93a] Kang et al. found that Mn(II) binding to serum albumin in blood induces a 10-fold enhancement in relaxivity.[93b] Koenig et al. measured NMRD profiles of liver and kidney tissue after injection of Mn(II) (or weakly chelated complexes) and found peaks in relaxation rate centered at ~10–20 MHz, indicative of Mn(II) in slowly tumbling environments, possibly bound to proteins or membrane surfaces.[94] The field dependence of relaxation is thus valuable in that it can qualitatively indicate binding interactions in tissue without independent determinations of agent concentration.

C. Parameters For Relaxivity Optimization

This section discusses each of the physical and chemical parameters important in relaxivity with regard to how they might be optimized to increase the efficiency of paramagnetic agents and thereby minimize the effective dose. This discussion is most relevant to the development of Gd(III), Mn(II), and Fe(III) contrast agents, since these ions generally have the highest relaxivity by virtue of large magnetic moments and long T_{1e}'s. The first two parameters discussed, r and q, are important in governing the strength of the electron–nuclear dipolar interaction. The parameters τ_R and T_{1e} in part determine the time scale of the fluctuations in the unpaired electron's magnetic field at the nucleus and are included in the spectral density portion of the Solomon–Bloembergen equations. Finally, τ_M can be important in modulating either the spectral densities or the efficiency of the chemical exchange of water

between chelate-bound and bulk environments.

1. Number of Coordinated Water Molecules, q

An early notion in NMR contrast agent design was that there existed a fundamental trade-off between relaxivity on one hand and stability and toxicity on the other: chelation of a metal ion with a multidentate ligand, while forming a stable and preferably nontoxic complex, leads to an enormous decrease in relaxivity largely due to the loss of some, if not all, of the coordinated water molecules. The higher doses of such a chelate necessary to alter tissue relaxation rates would partially offset its increased safety.

The paramount importance of safety in diagnostic examinations makes this "trade-off" idea irrelevant: complexes must be safe at their effective doses and, to prevent chronic effects, they must not dissociate to any appreciable degree in vivo. The demands of stability as well as targeting may sometimes be more important than relaxivity, as in the introduction of coordinatively saturated (outer-sphere relaxing) Fe(III) complexes as hepatobiliary agents by our group (see section VIIB).

Certainly, the presence of at least one coordinated water molecule (i.e., inner-sphere relaxivity) is important in attaining the high relaxivities on the order of 20–200 mM^{-1} s^{-1} that occur only for slowly rotating Gd(III) and Mn(II) systems. While outer-sphere relaxivity may be enhanced to some degree upon immobilization (by a factor of two or so), it will be limited to any further increase by the very rapid translational diffusion of water or transient hydrogen-bond lifetimes (~10 ps). Strategies pointed toward increasing the number of hydrogen-bonding sites in the second coordination sphere (q') or their residence time would nevertheless be welcome in optimizing relaxivity of complexes that are limited to the outer-sphere mechanism by the nature of the ligand.

2. Distance between the Water Protons and the Unpaired Electron Spin, r

The $1/r^6$ dependence in dipolar interactions presents the opportunity to increase relaxivity by (1) chemically inducing an orientation of bound water molecules such that the protons are closer to the metal center or unpaired spin density; or (2) delocalizing the unpaired spin density toward the water through atomic or molecular orbitals of the metal ion, the chelating ligand, or the bound water itself.

Waysbort and Navon pointed out that tilting of the plane of a bound water molecule with respect to the metal–oxygen vector would decrease r and increase relaxivity.[95] Neutron diffraction studies of transition-metal hydrates revealed that this indeed occurs in the solid state.[96] Two general classes of transition-metal-coordinated waters seem to exist: one where the tilt angle is 0–30° (class 1) and another with 36–55° tilt, where the dominant interaction is with only one of the oxygen lone pairs (class 1′). One-third of the relevant examples are members of this latter category. For Mn(II), the tilting can reduce the metal–proton distance roughly 0.2 Å, generating 50% greater relaxivity. Such an orientation of bound waters (55° tilt) has also been detected in neodymium(III) chloride solutions.[97] However, strategies to obtain a 55° tilt on a bound water, such as supplying an additional group on the chelate that would hydrogen bond to the remaining oxygen lone pair, have not been examined, and it seems unlikely that one can control such subtle structural features.

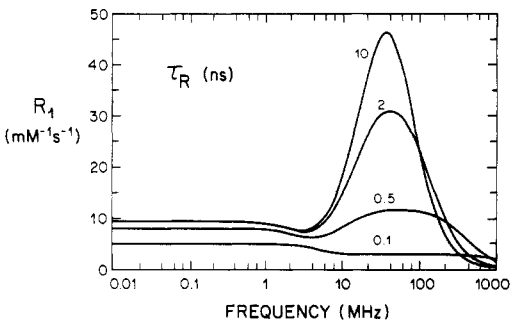

Figure 4. Calculated inner-sphere longitudinal relaxivities vs. Larmor frequency, or NMRD profiles, for different values of the rotational correlation time τ_R as shown. The Solomon–Bloembergen–Morgan (SBM) theory (eq 4–8, dipolar contribution only) was utilized with values for the other parameters typical of Gd(III) complexes: $S = {}^7/_2$, $q = 1$, $r = 3.13$ Å, $\tau_M = 3$ ns, $\tau_{S0} = 0.1$ ns, and $\tau_V = 40$ ps. The lowest value of τ_R chosen, 0.1 ns, is roughly that of low molecular weight complexes such as $[Gd(DTPA)(H_2O)]^{2-}$; the single dispersion at ~5 MHz is that of the "$7\tau_c$" term in eq 5 (the $3\tau_c$ term does not disperse under these conditions until ~1000 MHz). Increasing τ_R allows the frequency dependence of T_{1e} to be expressed (eq 8); with the value of τ_V chosen, T_{1e} increases dramatically with increasing frequency at ~10 MHz, creating the peak characteristic of slowly rotating paramagnetic ions. The increase in τ_c pushes the $7\tau_c$ dispersion to lower frequency (~2 MHz) and brings the $3\tau_c$ dispersion down to ~100 MHz. With the parameters used here, increasing τ_R above 10 ns does not increase relaxivity further since T_{1e} and/or τ_M become the dominant correlation times.

On the other hand, it appears more likely that the unpaired electron can be brought closer to the water protons. The foremost example is $[Mn^{III}(TPPS)(H_2O)_2]^{3-}$, where the observed relaxivity is three times that expected on the basis of the analogous Fe(III) complex (which has $q = 1$).[73] In this case, the nonspherical unpaired electron density of the d^4 manganese(III) ion, in which the d_{xz}, d_{yz}, d_{xy}, and d_{z^2} orbitals are occupied, was thought to be greatest along the z axis and, thus, somewhat closer to the protons on the axially coordinated water molecules. The effect is absent for the Fe(III) complex, where all orbitals are singly occupied. However, the structures of the two complexes in solution are different: the Mn(III) ion sits directly in the porphyrin plane, whereas the Fe(III) complex is thought to be pentacoordinate with the ion above the plane. The possible effects of this structural difference and delocalization of unpaired spin density onto the porphyrin ligand were not discussed. It will be important to distinguish between these different mechanisms since they imply separate strategies for relaxivity enhancement.

3. Rotational Correlation Time, τ_R

For metal ions with long T_{1e}'s, alteration of the rotational tumbling time τ_R is the single most important source of relaxivity enhancement. The degree of enhancement possible, which is limited by the values of T_{1e} and τ_M according to eq 6, exceeds that which is realistically available from optimizing any of the other relevant parameters. Figure 4 shows NMRD profiles as a function of τ_R calculated from the Solomon–Bloembergen and Bloembergen–Morgan equations. Parameters typical of Gd(III) are utilized. The enhance-

ment in R_1 predicted at longer τ_R values has been experimentally observed, as was shown in Table II. The enhancement has also been observed in viscous solvent mixtures containing paramagnetic metal ions.[98,99]

Three basic strategies exist to reduce the rotational mobility of metal complexes in vivo: (1) Distribution of the agent into a tissue or tissue compartment with high microviscosity. (2) Covalent attachment of the complex to a larger molecule such as a protein or antibody before injection. (3) Noncovalent binding of the complex in tissue to macromolecules.

The first of these ideas is important, not so much as a direct strategy for the present but more toward understanding the relaxivity of metal chelates in tissue. Debye–Stokes theory predicts that for a spherical molecule of radius a, τ_R is directly proportional to the viscosity of the medium, η, and the third power of the radius as given by eq 12, where k is the Boltzmann

$$\tau_R = 4\pi a^3 \eta / 3kT \qquad (12)$$

constant and T is the absolute temperature. Thus, the relaxivity of a complex should be directly proportional to η until τ_R approaches the value of T_{1e} and/or τ_M. James has discussed the problem of using the viscosity parameter η, which relates to macroscopic *translational* properties, to predict τ_R; a knowledge of *rotational* microviscosity, which unfortunately is less understood, is actually required to accurately estimate τ_R.[100]

As discussed in section IIIB4, the relaxivities of hydrophilic chelates like $[Gd(DTPA)(H_2O)]^{2-}$, which localize primarily in the intravascular and interstitial compartments of tissue, appear to be similar to the relaxivities observed in aqueous solution. This implies that the rotational microviscosity for molecules of this size is unchanged in these compartments despite the protein and cell content and extracellular matrix structures. On the other hand, intracellular environments do appear to exhibit higher microviscosity. EPR, NMR, and fluorescence studies of low molecular weight probes in mammalian cells reveal increases in τ_R ranging from two- to five- or tenfold relative to aqueous solution.[101] (The more recent work tends to favor the lower values.) The development of metal complexes that can safely sample cytosolic or other high-viscosity environments prior to excretion may offer an opportunity for modest increases in relaxivity.

The largest gains in relaxivity are possible through covalent or noncovalent attachment of a chelate to a macromolecule. Protein molecules, for example, generally have τ_R's of 10 ns or longer. Rigidly attached chelates experiencing this tumbling behavior would exhibit the highest possible relaxivity, as shown in Figure 4, limited largely by the values of T_{1e} and τ_M.

Any motion of the chelate independent of the macromolecule, however, can reduce relaxivity considerably. Dwek[13] and Burton et al.[15] discussed the possible effect of anisotropic (internal) rotation on relaxivity in paramagnetic protein–metal ion complexes. The simplified theory of Woessner,[102] which describes nuclear relaxation rates in the presence of internal motion about a single axis, is generally invoked. The decrease in relaxivity due to the internal motion is a function of its frequency and amplitude in addition to the position of the nucleus relative to the rotation axis. Metal-binding sites in metalloproteins usually have two or more attachment sites to the protein via amino acid residues and thus are likely to be well anchored. Segmental flexibility or other internal motions of proteins, well documented by a number of techniques,[103] would be the main source of relaxivity in this case. Due to the complex nature of anisotropic rotation and the number of parameters involved in relaxivity alone, NMR relaxation studies of metalloproteins have not provided evidence for internal motion at metal-binding sites. Nevertheless, it is possible that the neglect of these considerations may have contributed in some way to the failure of solvent relaxation rate measurements to provide unambiguous characterization.

The importance of internal motion of metal chelates attached to proteins is likely to be greater that in the metalloprotein case. For example, covalent attachment via lysine side chains, as described in section VB3, obviously leads to some degree of internal flexibility through the four methylene groups; the correlation time of the ϵ-CH_2 group in proteins has been estimated by ^{13}C NMR to be 0.4–1.5 ns.[104] It is not known whether the covalently attached aminocarboxylate chelates exhibit independent motion, although their relaxitivies seem somewhat lower than the metalloprotein complexes.

The case of metal complexes bound noncovalently to proteins has received little attention. The relaxivity enhancement may depend on the number of attachment points to the protein. Since the protein–chelate binding energies are likely to be determined by a number of relatively small contributions (such as electrostatic, hydrogen-bonding, van der Waals, and hydrophobic forces) from different groups on the complex, these interactions may result in less internal flexibility and higher relaxivity than when the chelate is attached to a single residue on the protein surface. EPR spectra of nitroxide spin labels bound either covalently or noncovalently to proteins show the latter to be the most rigidly immobilized.[105]

We have observed substantial relaxivity enhancement of iron(III)–*N*,*N*′-ethylenebis[(5-X-2-hydroxyphenyl)-glycinate] [Fe(5-X-EHPG)$^-$] (X = Cl, Br, I, CH_3, *t*-Bu; see section VIIB for structure) and Fe(III)–*N*,*N*′-bis-(2-hydroxybenzyl)ethylenediaminediacetate [Fe-(HBED)$^-$] complexes upon binding noncovalently to human serum albumin (HSA).[106,107] This enhancement (roughly two to four times the free relaxivities) occurs despite the fact that the complexes are coordinatively saturated and therefore outer-sphere relaxation agents. The greater part of the relaxivity probably stems from hydrogen-bonded water molecules in the second coordination sphere. If the relaxivity enhancement upon binding is due to an increase in τ_R and/or T_{1e} then the exchange lifetime of these waters (τ_M') cannot be considerably less than the values of the other correlation times in the free state.

The relative merits of covalent or noncovalent attachment of a chelate to a macromolecule to exploit the PRE effect are linked to targeting and toxicity considerations. The stable covalent linkage is favorable for labeling possible targeting macromolecules, such as monoclonal antibodies for imaging tumors or infarcted heart tissue and HSA for imaging blood vessels or tissue perfusion. However, the metabolism of such conjugates may present toxicity problems. For example, proteo-

lytic degradation occurs in lysosomes where the pH is sufficiently low (~4–5) such that the metal ions may dissociate from the chelate and exert toxic effects. The degradation of the chelate may be harmful as well. These potential complications, in addition to possible allergic reactions to the foreign protein (including multiply-labeled human proteins), may prevent the use of such conjugates at the dose necessary for NMR contrast enhancement.

The reversible, noncovalent binding of a chelate in vivo is a more attractive alternative. A fraction of the administered chelate would be bound to a particular site, inducing higher relaxivity, and this fraction would be in continuous equilibrium with the free (unbound) chelate. The free chelate would be safely excreted via the normal excretory mechanisms for small molecules, eventually shifting the equilibrium away from the bound species. Additionally, the binding could be directed toward specific target sites in the particular tissue of interest. The use of a noninvasive imaging technique such as NMR linked with an appropriate targeted agent would allow the novel opportunity to "visualize" binding events in vivo. The design of such complexes and the elucidation of their interactions with proteins is an area that deserves more attention (see section VII).

4. Electron Spin Relaxation Time, T_{1e}

The choice of Gd(III), Mn(II), and Fe(III) as optimal relaxation agents stem from their long T_{1e}'s and large magnetic moments. In these ions with stable, half-filled d or f shells, the pathways for electronic relaxation are relatively inefficient compared with other electronic configurations.[26] In general, increasing T_{1e} will yield higher relaxivity, limited by the values of τ_M, τ_R, or the correlation time for internal motions.

No comprehensive theory for electron spin relaxation of metal ions in solution has been presented. It is nonetheless instructive to consider the Bloembergen–Morgan (BM) theory (eq 8) derived for the aquo ions. Collisions between the chelate and solvent molecules are thought to induce a transient zero-field splitting (ZFS) of the spin levels. The electronic relaxation rate is related to the induced ZFS and a spectral density term, $f(\tau_V)$, where τ_V is the correlation time characterizing the ZFS modulation. Though this approach cannot be extended directly to less symmetrical metal complexes, the relationship between ZFS and T_{1e} is thought to be general: an increase in ZFS will lead to shorter T_{1e} values and reduced relaxivity. Figures 5 and 6 show calculated NMRD profiles illustrating this dependence for freely rotating and immobilized chelates. In these figures, we express the ZFS dependence in terms of its effect on T_{1e} at zero field, τ_{S0} ($\tau_{S0} = \tau_V/5B$, where B is the ZFS constant described in eq 8).

The need for long T_{1e}'s therefore translates into a desire to minimize ZFS in metal complexes. It may be possible to tune this parameter through changes in ligand field strength and symmetry. For example, La Mar and Walker have shown that the ^{1}H NMR line widths of Fe(III)–porphyrin complexes, which are sensitive to T_{1e}, are dependent on the donor strength of the axial ligand and the resulting ZFS in a manner consistent with BM-type theory.[108] The dependence of the outer-sphere relaxivity of Fe(5-X-EHPG)$^-$ complexes,

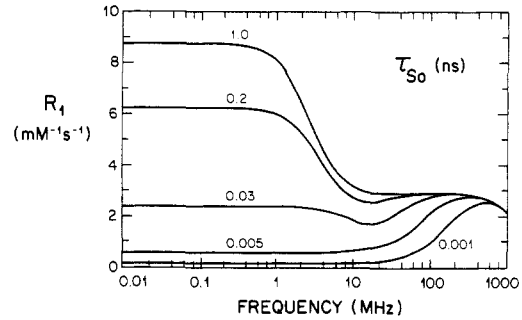

Figure 5. Calculated NMRD profiles for different values of T_{1e} at zero field (τ_{S0}) as shown for a freely rotating complex (τ_R = 0.1 ns). SBM theory was utilized with values for the other parameters typical of Gd(III) complexes: $S = {}^7/_2$, $q = 1$, $r = 3.13$ Å, $\tau_M = 3$ ns, and $\tau_V = 10$ ps. With long values of τ_{S0} (characteristic of Mn(II) and Gd(III)), τ_R is the dominant correlation time and a simple $7\tau_c$ dispersion is observed at ~2 MHz. As τ_{S0} decreases (or the zero-field splitting increases), this dispersion moves to higher frequencies, and the rise in relaxivity due to the frequency dependence of T_{1e} becomes evident at ~20–80 MHz; these intermediate curves have been observed experimentally for some Gd(III), Fe(III) and Cr(III) complexes.[28,69] When τ_{S0} is quite short (~10 ps or less), the $7\tau_c$ dispersion merges with the rise in relaxivity, creating an NMRD curve characterized by a single peak; this has been observed for aqueous Ni(II) solutions[99] and Mn(III)–porphyrin complexes.[73]

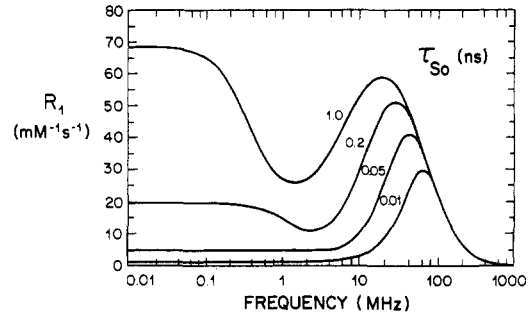

Figure 6. Calculated NMRD profiles for different values of T_{1e} at zero field (τ_{S0}) as shown for an immobilized complex (τ_R = 10 ns). SBM theory was utilized with values for the other parameters typical of Gd(III) complexes: $S = {}^7/_2$, $q = 1$, $r = 3.13$ Å, τ_M = 3 ns, and $\tau_V = 40$ ps. The results are qualitatively similar to that for freely rotating complexes (Figure 5) except that the peak in relaxivity is always present.

both free and bound to HSA, on the electron-donating or -withdrawing nature of the 5-substituent may result from similar changes in ZFS modulated through the donor strength of the coordinated phenolate.[106,107] While Mn(II) should be sensitive to these ligand field effects, Gd(III), with its buried 4f electrons, may not. Clearly, more work in this general area is necessary.

Electron spin relaxation in metal complexes with static ZFS may be modulated by both τ_R and τ_V. The interdependence of these parameters is not well understood (see section VA2). The exact nature of τ_V, i.e., what it physically represents, is not known in the case of metal chelates or metal–protein complexes. The value of τ_V determines the magnetic field strength at which T_{1e} begins to increase with field ($1/T_{1e}$ disperses away with field much like R_1). The onset of this phenomenon generates the characteristic peak in NMRD profiles of immobilized systems. Figure 7 illustrates that alterations in τ_V affect the magnitude of the peak and its position with respect to field.

While the nature of τ_V and the accuracy of various experimentally determined estimates are in question, this correlation time appears to be relatively inde-

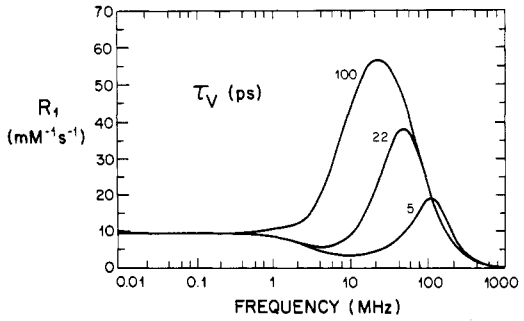

Figure 7. Calculated NMRD profiles for different values of τ_V as shown for an immobilized complex (τ_R = 10 ns). SBM theory was utilized with values for the other parameters typical of Gd(III) complexes: $S = {}^7/_2$, $q = 1$, $r = 3.13$ Å, $\tau_{S0} = 0.1$ ns, and $\tau_M = 3$ ns.

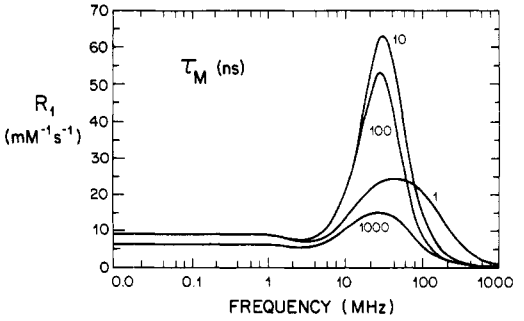

Figure 8. Calculated NMRD profiles for different values of τ_M as shown for an immobilized complex (τ_R = 10 ns). SBM theory was utilized with values for the other parameters typical of Gd(III) complexes: $S = {}^7/_2$, $q = 1$, $r = 3.13$ Å, $\tau_{S0} = 0.1$ ns, and $\tau_V = 40$ ps.

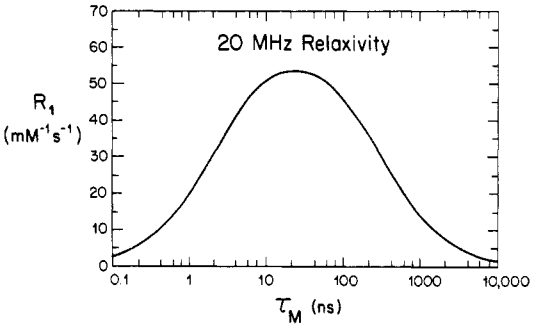

Figure 9. Calculated relaxivity at 20 MHz (SBM theory) as a function of τ_M for an immobilized complex (τ_R = 10 ns). Parameters typical of Gd(III) complexes were chosen: $S = {}^7/_2$, $q = 1$, $r = 3.13$ Å, $\tau_{S0} = 0.1$ ns, and $\tau_V = 40$ ps.

pendent of the particular metal ion, most likely relating to fluctuations at the primary coordination sphere induced by solvent collisions. Koenig and co-workers have noted that protein–metal ion complexes, which may be somewhat shielded from solvent, exhibit longer τ_V values (20–50 ps) compared with those of the aquo ions (~5 ps).[73] More interesting is their finding that porphyrin complexes, which are quite rigid in the equatorial plane, exhibit long τ_V's (30 ps);[73] perhaps this relates to the reduced tendency of solvent collisions to distort the coordinated nitrogens.

5. Residence Lifetime of Coordinated Waters, τ_M

The residence lifetime, τ_M, has a dual importance in relaxivity: it can contribute to the overall correlation time, τ_c (eq 6), and it modulates the efficiency of the chemical exchange of water molecules sampling the paramagnetic center (eq 4). The lability of monodentate metal–ligand bonds in complexes of ions with no ligand field stabilization energy, such as those of Gd(III), Mn(II), and Fe(III), results in short τ_M values on the order of 1 ns–1 μs.

For freely rotating complexes of these ions, τ_R dominates τ_c, and T_{1M} values are approximately 10–100 μs. Thus, τ_M is not generally a factor in the spectral density terms, and fast-exchange conditions prevail ($\tau_M \ll T_{1M}$) with no dependence on τ_M.

The exchange lifetime does, however, have importance as a final optimization parameter for immobilized systems. If short, τ_M can have the same order of magnitude as τ_R and T_{1e} and thus reduce relaxivity, especially at higher fields where T_{1e} increases. Alternatively, T_{1M} values in these more efficiently relaxing conditions are somewhat shorter than when freely tumbling. The intermediate exchange condition ($\tau_M \sim T_{1M}$), which yields lower relaxivity than the fast-exchange case, becomes possible if τ_M is long. The result of these possibilities is a parabolic dependence of relaxivity on τ_M, as illustrated in Figures 8 and 9.

The binding of a metal chelate to a protein could influence the exchange time directly, via hydrogen-bonding interactions with the bound water or steric blocking of the water exchange pathway to the bulk solvent, or indirectly, via alteration of the multidentate ligand structure and/or the primary coordination sphere. τ_M values in metalloproteins have been estimated in the range of 1 ns–1 μs.[15] Little is known concerning how the protein influences the exchange in each case. Similarly, it is difficult to predict whether protein binding of chelates influences τ_M. If intermediate exchange does occur with concomitant relaxivity reduction, then specific strategies may become important, such as altering the chelate orientation in the protein binding site to allow for free water exchange.

On the other hand, if the structure of the chelate is rate determining, it may be possible to tune this exchange rate for maximum relaxivity. The current understanding of water exchange in metal chelates, though still at an early stage, has stemmed largely from the ^{17}O NMR technique for estimating τ_M developed by Swift and Connick.[109] The contact shift and transverse relaxation rate of $H_2{}^{17}O$ in the presence of dissolved paramagnetic ions is related to τ_M as described by the scalar portion of the Solomon–Bloembergen equations. Table III lists reported values of τ_M obtained by this technique for aquo ions and complexes pertinent to the development of contrast agents. The results of Hunt and co-workers on a wide variety of nickel(II) complexes is also included for discussion.[110–113]

In all but the Gd(III) examples, substitution of waters by stronger and/or anionic donor ligands labilizes the metal–water bond. This labilizing effect has been discussed by Margerum et al. in their comprehensive review of coordination chemistry kinetics.[114] For the Ni(II) complexes, τ_M decreases as the σ-donating strength of the other ligands increases. The π-back-bonding ligands such as bpy seem to have less of a labilizing effect. The decrease in τ_M observed for Ni(II), Mn(II), and Fe(III) ternary complexes relative to their aquo ions is reasonable in view of the longer M–OH_2 bond lengths in the former.

A sufficient number of τ_M values for complexes of different structure have not been obtained in order to

TABLE III. Residence Lifetime (τ_M) of Primary Coordination Sphere Water Molecules as Calculated from ^{17}O NMR Relaxation Data.

complex	τ_M, ns	ref
$Gd(H_2O)_n^{3+}$ (n = 8, 9)	0.94	116
$Gd(PDTA)(H_2O)_2^-$	3.0	116
$Mn(H_2O)_6^{2+}$	43 000	114
$Mn(phen)(H_2O)_4^{2+}$	19	114
$Mn(phen)_2(H_2O)_2^{2+}$	8.3	114
$Mn(ATP)(H_2O)_n^{2-}$	20	114
$Mn(EDTA)(H_2O)^{2-}$	2.3	114
$Mn(NTA)(H_2O)_2^-$	0.67	114
$Fe(H_2O)_6^{3+}$	5.3×10^6	*a*
$Fe(H_2O)_5(OH)^{2+}$	8300	*a*
$Fe(EDTA)(H_2O)^-$	1300	75
$Fe(TMPyP)(H_2O)_n^+$	1300	115
$Fe(TPPS)(H_2O)_n^{3-}$	71	115
$Ni(H_2O)_6^{2+}$	32 000	113
$Ni(terpy)(H_2O)_3^{2+}$	19 000	110
$Ni(bipy)(H_2O)_4^{2+}$	20 000	110
$Ni(bipy)_2(H_2O)_2^{2+}$	15 000	110
$Ni(EDDA)(H_2O)_2$	5600	114
$Ni(HEDTA)(H_2O)^-$	5000	114
$Ni(EDTA)(H_2O)^{2-}$	1400	114
$Ni(H_2O)_5Cl^+$	7100	114
$NiNH_3(H_2O)_5^{2+}$	4000	110
$Ni(NH_3)_2(H_2O)_4^{2+}$	1600	110
$Ni(NH_3)_3(H_2O)_3^{2+}$	400	110
$Ni(en)(H_2O)_4^{2+}$	2300	110
$Ni(en)_2(H_2O)_2^{2+}$	190	110
$Ni(dien)(H_2O)_3^{2+}$	29 000, 2300[b]	112
$Ni(trien)(H_2O)_2^{2+}$	1800	112
$Ni(tetren)(H_2O)^{2+}$	89	112
$Ni([12]aneN_4)(H_2O)_2^{2+}$	48	113

[a] Grant, M.; Jordan, R. B. *Inorg. Chem.* **1981**, *20*, 55. [b] Two classes of exchanging waters.

rationally approach the idea of "tuning τ_M" for maximum relaxivity. The existing data, however, do reveal some interesting effects. Macrocyclic ligands seem to have large labilizing effects, as observed for the Fe(III) porphyrin[115] and Ni(II)[14]aneN[113] complexes. The lower τ_M observed for Fe(TPPS) compared with Fe(TMPyP) (71 and 1300 ns, respectively) was interpreted as resulting from more charge donation in the former, suggesting that in some cases simple remote substitutions might be sufficient to tune τ_M.

The effect of coordinated carboxylates on τ_M, which is important due to the prevalence of such groups in potential contrast agents, is not clear. Merbach and co-workers reported that the PDTA ligand does not appear to have the customary labilizing effect when coordinated to Gd(III).[116] Their estimated τ_M values for the Gd(III) aquo ion and $[Gd(PDTA)(H_2O)_2]^-$ of 0.94 and 3.0 ns, respectively, show the opposite trend. This increase in τ_M upon complexation appears to be in disagreement with the increased M–OH_2 bond length expected for the PDTA complex; e.g., this distance increases from 2.49 to 2.57 Å upon complexation of $Nd^{III}(H_2O)_9^{3+}$ with DTPA to form $[Nd(DTPA)(H_2O)]^{2-}$.[79,117] Merbach and co-workers suggest that hydrogen bonds between the protons of the coordinated water and the acetate oxygens might be responsible for the longer τ_M of $[Gd(PDTA)(H_2O)_2]^-$. It is interesting that carboxylates apparently have a similar effect on the τ_M's of Ni(II) complexes. The τ_M for $Ni(EDDA)(H_2O)_2$ (5.6 μs) is longer than that of either $Ni(en)(H_2O)_4^{2+}$ (2.3 μs) or $Ni(trien)(H_2O)_2^{2+}$ (1.8 μs).[114] One of course has to wonder about the accuracy of these experimentally determined values (especially in view of the limitations of the Solomon–Bloembergen–Morgan equations) and the feasibility and strength of the nonlinear hydrogen bonds proposed.

VI. Stability and Toxicity

The acute and chronic toxic effects of paramagnetic metal complexes will be important to understand in view of the likely possibility of routine intravenous administration of such compounds for NMR imaging examinations in the future. The required doses of such compounds (roughly 0.5–5 g per patient) greatly exceeds that of metal ions or complexes used in radioscintigraphy. However, iodine-containing contrast agents are used in computed tomography (CT) and other radiological procedures at much higher doses than NMR agents (~50–200 g per patient). With the development of relatively nontoxic chelates, the contrast-enhanced NMR exam is likely to be safer than similar CT procedures.

Toxicity and stability are discussed togther here to emphasize the historical importance of metal complex stability in determining toxicity in early evaluations of NMR agents. The dissociation of a complex generally leads to a higher degree of toxicity stemming from the free metal ion or free chelating ligand. While the testing and mechanistic understanding of metal complex toxicity requires the expertise of toxicologists and pharmacologists, the chemist can contribute tremendously to the development of safe chelates, largely by synthesis of more stable derivatives and elucidation of dissociation mechanisms in biological conditions.

A. Toxicity of Metal Complexes

Toxic effects from a metal complex can arise from (i) free metal ion, released by dissociation; (ii) free ligand, which also arises from dissociation; and (iii) the intact metal complex. In the latter two cases, one may also have to consider metabolites that may be more toxic than the parent compound.

The available toxicological data point to the importance of metal complex dissociation as an important source of toxicity. Table IV lists acute LD_{50} values (interpolated dose at which 50% of the animals would die) determined for metal ions, complexes, and ligands. Both metal ions and free ligands tend to be more toxic than metal chelates. This is reasonable if one considers that complexation itself "neutralizes" the coordinating properties of both the ligand and the metal ion to some degree, decreasing their avidity for binding to proteins, enzymes, or membranes via electrostatic or hydrogen-bonding interactions or covalent bonds.

In the simplest view, the degree of toxicity of a metal chelate is related to its degree of dissociation in vivo before excretion. A good example of how toxicity and in vivo stability depend on the chelating ligand is the comparison between $[Gd(EDTA)(H_2O)_n]^-$ and $[Gd(DTPA)(H_2O)]^{2-}$. The latter is a very stable complex ($\log K_{ML}$ = 22.5) that is excreted intact readily by the kidneys, exhibiting a very low degree of toxicity (LD_{50} 10–20 mmol/kg).[118] $[Gd(EDTA)(H_2O)_n]^-$, on the other hand, has a toxicity comparable to $GdCl_3$ (LD_{50} ~ 0.5 mmol/kg) despite its apparently high thermodynamic stability ($\log K_{ML}$ = 17.4).[118] The straightforward interpretation is that the latter complex quantitatively dissociates in vivo, yielding the toxicity of the free ion.

TABLE IV. Acute LD_{50} Values for Metal Salts, Metal Complexes, and Free Ligands

compound	LD_{50}, mmol/kg	animal	admin[a]	ref
$GdCl_3$	0.5	rat	iv	118
	0.4	mouse	iv	7, 89
	0.26	rat	iv	4
	1.4	mouse	ip	*b*
$Gd(OH)_3$	0.1	mouse	iv	7, 89
(MEG)[Gd(EDTA)$(H_2O)_n$][c]	0.3	rat	iv	118
	0.62	mouse	ip	*b*
MEG[Gd(CDTA)$(H_2O)_n$]	<2.5	rat	iv	*d*
MEG[Gd(EGTA)$(H_2O)_n$]	<2.5	rat	iv	*d*
$(MEG)_2$[Gd(DTPA)(H_2O)]	10	rat	iv	118
	>10	mouse	iv	89
Na_2[Gd(DTPA)(H_2O)]	>10	mouse	iv	7
	20	rat	iv	4
(MEG)[Gd(DOTA)(H_2O)]	>10	mouse	iv	89
Na[Gd(DOTA)(H_2O)]	>10	mouse	iv	89
$(MEG)_3$[Gd(TTHA)]	6	rat	iv	*d*
$MnCl_2$	0.22	rat	iv	4
	1.5	mouse	ip	*b*
Na_2[Mn(EDTA)(H_2O)]	7.0	rat	iv	4
	5.9	mouse	ip	*b*
Na_3[Mn(DTPA)]	1.9	rat	iv	4
Mn(III)$(TPPS)^{3-}$	~0.5	mouse	iv	120
$FeCl_3$	1.6	mouse	ip	*b*
Na[Fe(EDTA)(H_2O)]	3.4	mouse	iv	89
	1.7	mouse	ip	*b*
Na_3[Ca(DTPA)]	5.0	rat	iv	4
	3.5	mouse	iv	7
$(MEG)_3H_2$DTPA	0.15	mouse	iv	89
Na_2H_3DTPA	0.1	mouse	iv	7
Na_2[Ca(DOTA)]	>7.0	mouse	iv	*e*
$(MEG)_2H_2$DOTA	0.18	mouse	iv	89

[a] Route of administration: iv = intraveneous; ip = intraperitoneal. [b] *Registry of Toxic Effects of Chemical Substances*; National Institute of Occupational Safety and Health; U.S. Government Printing Office: Washington, DC, 1982. [c] MEG = *N*-methylglucamine. [d] Weinmann, H.-J., unpublished results. [e] Tweedle, M. F., unpublished results.

The driving force for this dissociation will be discussed in the next section.

The toxicity of metal ions has been extensively reviewed.[119] The coordination of ions to oxygen, nitrogen, or sulfur heteroatoms in macromolecules and membranes alters the dynamic equilibria necessary to sustain life. Gd(III), for example, can bind to Ca(II) binding sites, often with higher affinity, owing to its greater charge/radius ratio.

The toxicity of free ligands, which is less understood, can stem from the sequestration of essential metal ions such as Ca(II) in addition to "organic" toxicity.

The toxicity of intact metal complexes can stem from a wide variety of specific and nonspecific effects. At the high doses required in LD_{50} determinations of relatively nontoxic hydrophilic chelates like [Gd(DTPA)$(H_2O)]^{2-}$, the nonspecific hypertonic effect is thought to be important. A difference in osmolality between intracellular and extracellular compartments is established after injection of large quantities of the ionic complexes and appropriate counter ions. Water is drawn out of cells as a result of the osmotic gradient, causing cellular and circulatory damage.

Other possible mechanisms of chelate toxicity include enzyme inhibition, nonspecific protein conformational effects, or alteration of membrane potentials. The toxicity of Mn^{III}TPPS, for example, is likely to be due to the intact complex, since it is kinetically inert to dissociation.[120] The combination of a large planar and hydrophobic region with anionic groups on the periphery may impart an affinity for binding in vivo. The toxicity of the cationic Mn^{III}TMPyP is reported to be much greater,[120] perhaps due to the prevalence of negatively charged macromolecules (e.g., DNA) and cell surfaces to which binding occurs. The interactions between metal chelates and biological macromolecular structures, which are not well understood, represent an important area of investigation relevant to understanding toxicity on a molecular basis.

B. In Vivo Stability of Metal Complexes

The requirement of metal complex stability is specifically a kinetic, not thermodynamic, requirement. The agent should be efficiently excreted from the body minutes or hours after administration, and stability is therefore required only for this residence time. The presence of thermodynamic sinks other than the metal–ligand complex can certainly exist in biological environments; these states, however, will not be reached if the dissociation rate of the complex is sufficiently slow.

The spherical electronic distribution of Gd(III), Mn(II), and Fe(III), which leads to long T_{1e}'s and high relaxivity, is unfortunately detrimental to complex stability. The lack of ligand field stabilization energy in complexes of these ions leads, generally, to very labile metal–ligand bonds. Kinetic stability must therefore derive from the structure of an appropriate multidentate ligand. The dissociation kinetics are nevertheless related to the thermodynamics of complexation via the simple expression of eq 13, where k_a and k_d are the

$$k_d = k_a/K_{ML} \tag{13}$$

association and dissociation rate constants and K_{ML} is the thermodynamic association constant. Thermodynamic considerations are also important in identifying the source of instability.

Though a complex may encounter a number of tissue compartments in vivo, which may differ with respect to dissociation factors, serum stability is most often evaluated, as has been the practice in radiopharmaceutical applications of metal complexes. A variety of coordinating ligands and proteins as well as metal ions can compete for either the paramagnetic metal ion or its multidentate ligand, providing a suprisingly rigorous test of metal complex stability.

Martell discussed in detail the expected stability of Fe(III) complexes in serum from the point of view of designing sequestering ligands for the treatment of iron overload conditions.[121] Moerlein and Welch presented a similar analysis of gallium(III) and indium(III) complexes as radiopharmaceuticals.[122] Many similarities exist in the aqueous chemistry of these three trivalent ions. A similar treatment of Gd(III) complexes, however, has not been offered, and the following discussion summarizes the important points.

An important thermodynamic sink for trivalent metal ions in serum is their precipitation with commonly occurring anions like hydroxide, phosphate, or carbonate. Table V lists the available solubility product constants (K_{sp}) relevant for NMR contrast agent design. Also shown are calculated values of the free metal ion concentration in the presence of both the precipitate and appropriate concentrations of the anion in serum. Both phosphate and carbonate appear to be important

TABLE V. Relevant Solubility Product Constants (K_{sp}) and Calculated Free Concentrations of Gd(III), Fe(III), and Mn(II) in Serumlike Conditions

compound	log K_{sp}[a] (25 °C, μ = 0)	free metal ion concn, M[b]
$GdPO_4$	−22.26[c]	4×10^{-15}
$Gd_2(CO_3)_3$	−32.2	5×10^{-10}
$Gd(OH)_3$	−25.6	2×10^{-6}
$FePO_4$	−26.4	3×10^{-19}
$Fe(OH)_3$	−41.5	2×10^{-22}
$MnCO_3$	−9.3	2×10^{-5}
$Mn(OH)_2$	−12.8	2.5

[a] Martell, A. E.; Smith, R. M. *Critical Stability Constants*; Plenum: New York, 1974; Vol. 4. [b] Calculated from K_{sp}'s and protonation constants of the anions: pH = 7.4, $[HCO_3^-]$ = 27 mM, $[HPO_4^{2-} + H_2PO_4^-]$ = 2 mM. [c] μ = 0.5.

for the precipitation of Gd(III), whereas for Fe(III) the formation of the hydroxide complex is favored. Precipitation of Mn(II) does not appear to be a problem.

The calculation of whether a complex is thermodynamically stable to precipitation of the ion in serum can be approached from the opposite viewpoint, i.e., whether a ligand can solubilize the ion from the precipitate. Martell[121] defined the solubilization constant K_{sol} as the degree of conversion of the free ligand to the metal chelate where T_L is the total concentration of the ligand (eq 14). Low values of K_{sol} reveal an inability

$$K_{sol} = [ML]/T_L \quad (14)$$

of a ligand to solubilize the ion; alternatively, it would predict that the complex would be unstable with respect to metal ion precipitation. Very high values of K_{sol} would occur for a thermodynamically stable complex where no precipitate would be present.

Log K_{sol} can be calculated for complexes of single multidentate ligands from eq 15, which takes into account additional equilibria of the ligand. K_{ML} is the

$$\log K_{sol} = \log K_{ML} + \log [M]_{free} - \log (\alpha_L^{-1} + \alpha_{Ca}^{-1}) \quad (15)$$

formation constant of the completely ionized ligand for the metal ion, $[M]_{free}$ is the free metal ion concentration in the presence of the solid and precipitating anions (from Table VI), and the final term represents competing equilibria of the ligand due to protonation (α_L) or complexation with Ca(II) (α_{Ca}):

$$\alpha_L = (1 + [H^+]\beta_1^H + [H^+]^2\beta_2^H + \cdots [H^+]^n\beta_n^H)^{-1} \quad (16)$$

$$\alpha_{Ca} = ([Ca]K_{CaL})^{-1} \quad (17)$$

In eq 16 and 17, the β_n^H values represent the overall formation constants of protonated ligand species; K_{CaL} is the formation constant of the Ca(II) complex with the free concentration of Ca(II) set at 5 mM.

Calculated log K_{sol} values for various Fe(III) and Gd(III) complexes are shown in Table VI along with their K_{ML} values and those of the analogous Ca(II) chelates. The K_{sol} values for the Fe(III) complexes, based on competition with the precipitation of $Fe(OH)_3$, show that only the very stable EHPG and HBED chelates are truly thermodynamically stable at serum pH. When additional equilibria are taken into account, such as Fe(III) binding to transferrin, these complexes are still sufficiently stable.[121] Various synthetic and naturally occurring ligands studied by Raymond and co-workers exhibit even higher stability.[123] The EDTA and DTPA complexes of Fe(III) are predicted to be less

TABLE VI. Association Constants (K_{ML}) and Calculated Stability Constants in Serum with Respect to Precipitation (K_{sol})

ligand	Ca(II), log K_{ML}[a]	Gd(III), log K_{ML}	Gd(III), log K_{sol}[b]	Fe(III), log K_{ML}[a]	Fe(III), log K_{sol}[c]
EDTA	10.61	17.35[a]	−5.4	25.0	−3.81
DTPA	10.75	22.46[a]	−0.4	28.0	−0.95
TTHA	9.89	23[d]	1	26.8	−1.3
DOTA	17.23[e]	28[f]	−1		
		24.7[g]	−4.3		
TETA	8.32[e]	15.75[h]	−4.7		
EHPG	7.2	18.2[i]	−4.6	33.9	4.28
HBED	9.29			39.7	8.87

[a] 25 °C. Martell, A. E.; Smith, R. M. *Critical Stability Constants*; Plenum: New York, 1974; Vol. 4. [b] K_{sol} = $[ML]/[L]_{total}$ in the presence of $GdPO_4$ calculated from eq 14–17; pH = 7.4; $[HPO_4^{2-} + H_2PO_4^-]$ = 2 mM, [Ca(II)] = 5 mM. [c] Same as *b* except for $Fe(OH)_3$; ref 115. [d] Estimated from Sm(III) value. [e] Delgado, R.; Frausto da Silva, J. J. R. *Talanta* **1982**, *29*, 815. [f] Estimated from Eu(III) value, 20 °C. Loncin, M. F.; Desreux, J. F.; Merciny, E. *Inorg. Chem.* **1986**, *25*, 2646. [g] Cacheris, W. P.; Nickle, S. K.; Sherry, A. D. *Inorg. Chem.* **1987**, *26*, 958. [h] 80 °C, 1 M NaCl; from *f*. [i] Kiraly, R.; Balazs, M.; Brucher, E. *Mag. Kem. Foly.* **1978**, *84*, 211.

stable, as was calculated for the analogous complexes of Ga(III) and In(III). The fact that aminocarboxylate complexes such as these appear relatively stable in radiopharmaceutical applications testifies to a degree of kinetic inertness to exchange, perhaps due to the high charge/radius ratios of the ions and high K_{ML}'s of their complexes.[122]

The log K_{sol} values for the Gd(III) complexes are calculated assuming phosphate as the chief precipitating anion. The results are important in ascertaining the instability and toxicity of $[Gd(EDTA)(H_2O)_n]^-$. This complex has a very low value of log K_{sol} (−5.4) compared with the DTPA complex (−0.4); the latter has been observed to be stable in vivo.[118] This suggests that Gd(III) complexes with K_{ML} values lower than $[Gd(EDTA)(H_2O)_n]^-$ are not worth screening.

It is likely that, like the Fe(III)–aminocarboxylate complexes, dissociation kinetics are playing the dominant role in determining Gd(III) complex stability. The crystal structure of $[Gd(EDTA)(H_2O)_n]^-$ reveals that the ligand occupies roughly one hemisphere of the ion, leaving the other side relatively open for coordination by labilizing ligands or oxo-bridged dimer formation.[84] This is not the case for $[Gd(DTPA)(H_2O)]^{2-}$ where, based on the analogous neodymium(III) complex, only one open coordination site exists.[80] The higher denticity of DTPA most likely contributes to its kinetic stability.

$[Gd(DOTA)(H_2O)]^-$ has been observed to be stable in vivo, exhibiting biodistribution behavior similar to $[Gd(DTPA)(H_2O)]^{2-}$.[6] It is interesting that despite the higher K_{ML} for the DOTA complex (log K_{ML} ~ 25–28) compared with DTPA (log K_{ML} = 22.5), the calculated K_{sol} values for DOTA are less than those for DTPA. This is due in part to the high K_{ML} for $[Ca(DOTA)]^{2-}$, which depletes the free ligand concentration in these calculations employing physiological concentrations of Ca(II) (5 mM).

The dissociation kinetics of $[Gd(DOTA)(H_2O)]^-$ are extremely slow due to its conformational stability and macrocyclic nature. Desreux and co-workers studied the acid-catalyzed dissociation and obtained a k_d of 10^{-5} M^{-1} s^{-1}.[124] The half-life of the complex is estimated to be 11 days at pH 1 and over 2000 years at pH 6.

Gansow and co-workers performed serum stability studies for DOTA, DTPA, and substituted DTPA complexes of $^{153}Gd(III)$.[125] The radioactive complexes were incubated at 37 °C under a 95% air/5% CO_2 atmosphere to maintain bicarbonate concentration. Loss of Gd(III) from the complexes resulted in radioactive precipitates. Over the 125-h observation period, $[Gd(DOTA)(H_2O)]^-$ lost 5% or less radioactivity, whereas $[Gd(DTPA)(H_2O)]^{2-}$ lost 10–20%. These results indicate that the small degree of thermodynamic instability of the DOTA and DTPA complexes with respect to phosphate precipitation, as calculated above, may actually hold. (The extension of these results to predict in vivo stability is not straightforward. The investigators used a phosphate buffer in the preparation of the incubation samples, artificially raising the phosphate concentration and favoring $GdPO_4$ precipitation.) The difference observed between the two complexes in this long-term study most likely arises from dissociation kinetics. It is noteworthy that the Gd(III) complex of the DTPA derivative with a benzyl substituent on one ethylene had stability similar to that of the parent compound. In contrast, Meares and co-workers observed that similar substitutions of EDTA decreased the dissociation rate of $^{111}In(III)$ from this ligand.[126] The investigators attributed the apparent increased stability to steric effects, which decrease rearrangement and dissociation rates. Perhaps in the case of DTPA such substitutions are required on both ethylene groups to be effective in augmenting kinetic stability.

Serum stability studies for relevant Fe(III) and Mn(II) complexes have not been reported. The EHPG and HBED complexes of Fe(III) are expected to be stable on the basis of Table VI. We observed no evidence of dissociation of $Fe(EHPG)^-$ or its derivatives in NMR imaging or biodistribution studies; visible spectra showed that the $Fe(EHPG)^-$ complex was excreted intact into the bile of a rabbit.[127,128] Concerning Mn(II) complexes, the PDTA complex ($\log K_{ML} \sim 10$) is known to dissociate in vivo, though the mechanism is unknown.[94] It is possible that competing equilibria with Ca(II) ($\log K_{CaL} \sim 7$) and proteins or enzymes ($\log K_{eff} \sim 3$) are involved.

Mn(III)–porphyrin complexes are of interest because of their high relaxivities (see section VC2). Cohen and co-workers noted that $Mn^{III}TPPS$ was stable for 9 days in human plasma at pH 7.5.[120] NMRD profiles of excised tissue containing the complex seem to reflect only the complex and not free Mn(II) or Mn(II)–protein complexes [Mn(III)(aq) is reduced by water and therefore not likely to be present]. In contrast, another macrocyclic Mn(III) complex, $Mn^{III}([14]aneN_4)(H_2O)_2$ [$Mn(cyclam)(H_2O)_2$], may not be stable in vivo. Jackels et al.[129] estimated the effective relaxivity (6.25 MHz) of the complex in liver and kidney as 17 times greater than in aqueous solution, possibly arising from the reduction of the ion and dissociation of the complex (order unknown); the free Mn(II) would then bind to proteins, exhibiting high relaxivity.

For the design of improved NMR contrast agents, the area of metal complex stability deserves more attention. New synthetic methods toward kinetically inert complexes, especially those of Gd(III), need to be developed. These preferably should be versatile enough to allow for specific substitutions on the complex that may modulate its properties. In parallel, we also need to understand the factors governing kinetic stability of metal complexes in serum and other physiological environments. For example, how do simple substituents on the chelate alter dissociation kinetics? How do simple ligands in serum such as citrate or amino acids influence dissociation? The catalytic effect of such ligands has been found to be important in the exchange of Fe(III) with transferrin; strategies to prevent this catalysis in metal complexes may be fruitful.

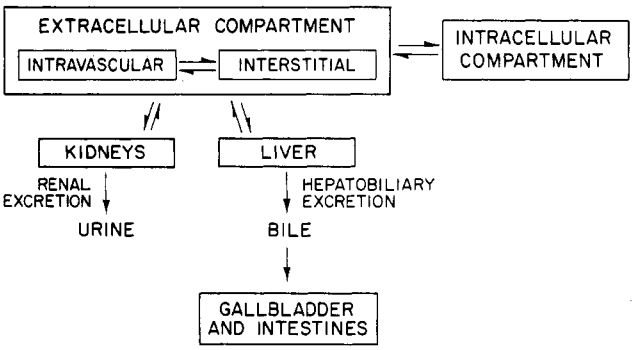

Figure 10. Principal distribution sites and excretion pathways for intravenously administered soluble metal complexes.

VII. In Vivo Targeting

Targeting a paramagnetic agent to a particular site within the body is one of the most challenging aspects of NMR contrast agent design. The diagnostic utility of a contrast-enhanced NMR imaging examination will depend on the absolute concentration of the agent in the desired tissue and the selectivity of the distribution relative to other tissues. True targeting is rarely achieved. After administration, the agent equilibrates in several body compartments prior to excretion; preferential distribution of the agent to the desired site is all that can be expected in most circumstances. NMR imaging agents are similar to radiopharmaceuticals or iodinated CT agents in that the NMR image enhancement depends on the concentration of a paramagnetic metal complex. The principles of distribution governing these other agents are directly applicable to NMR agents.

However, the dependence of relaxivity on the chemical environment of a paramagnetic complex alters this simple view. What is directly relevant to NMR imaging is not the actual distribution of the agent but the distribution of the relaxation rate changes induced by the agent. The enhancement in relaxivity induced by binding the agent to a macromolecule (the PRE effect) is of central importance. By targeting a complex to desired sites where such binding interactions occur, the target/nontarget ratios in terms of relaxation rate changes may be increased above that in terms of concentration. Little has been done to reduce this "binding-enhancement" concept to practice. A prerequisite for the development of such agents is a better understanding of protein–chelate binding. Our investigation of the noncovalent binding of $Fe(5\text{-}Br\text{-}EHPG)^-$ isomers by human serum albumin, discussed in section VIIB, is toward this goal.

Figure 10 illustrates potential distribution sites and excretion pathways relevant for soluble metal complexes. An intravenously administered chelate rapidly

equilibrates in the intravascular and interstitial (space between cells) fluid compartments; these collectively are referred to as the extracellular compartment. Depending on its structure, the complex may also distribute into various intracellular environments (including that of liver and kidney) by passive diffusion or specific uptake processes.

The structure of the complex determines its excretion pathway. Most commonly, small molecular weight hydrophilic chelates that do not bind to plasma proteins are nonspecifically filtered out in the kidneys (glomerular filtration).[130] If the molecule possesses a balance between hydrophobic and hydrophilic character, particularly if it contains aromatic rings, some fraction of the complex is taken up by liver cells and excreted into the bile (hepatobiliary excretion).[131] Such molecules often exhibit some degree of plasma protein binding, particularly to albumin, which reduces the free fraction available for glomerular filtration. The hepatobiliary and renal pathways can thus be competitive. Generally, the greater degree of lipophilicity a molecule possesses the greater the hepatobiliary excretion.[131] The complete clearance of the agent from the body by either route is of course desirable to minimize toxicity. If, however, the complex is very lipophilic, it can (1) distribution into fat storage sites or membranes or (2) precipitate in blood and be taken up by reticuloendothelial cells in the liver and spleen. Both possibilities lead to long-term retention of the agent, which may be associated with chronic toxicity.

The following is a discussion of the various classes of metal complexes under investigation as NMR imaging agents. Due to the relatively high concentration of a paramagnetic agent required for image enhancement, the targeting of low-concentration receptor sites (<1 μM), as in traditional radioscintigraphy or positron emission tomography,[132] is not feasible for NMR imaging. Therefore, the diagnostic utility of most of the complexes under examination is linked to their general distribution and/or excretion pathway, and this is reflected in the classifications below. The emphasis here is on the chemistry and biochemistry of the agents; only illustrative examples of diagnostic applications are offered. The reader is referred to other review articles and monographs for the radiological perspective.[3-7]

A. Extracellular Distribution: Renal Excretion

$[Gd(DTPA)(H_2O)]^{2-}$ and, more recently, $[Gd(DOTA)(H_2O)]^-$ are prototype complexes of this class of agents.[6,7,118,133] Compared with other substances discussed below, these agents are referred to as nonspecific in reference to their nonselective extracellular distribution. Their localization in tissues does not usually reflect specific cellular processes. They nevertheless form an important class of potential NMR agents that resemble iodinated CT contrast media as well as more analogous radiopharmaceuticals such as the DTPA complexes of ^{99m}Tc or ^{113}In.[132]

The structural requirements for these agents are satisfied by simple metal complexes. The presence of charged or hydrogen-bonding groups such as carboxylates and the lack of large hydrophobic groups ensure minimum interaction with plasma proteins, other macromolecules, and membranes. This allows for the equilibration of the complex in the extracellular space and efficient renal excretion. The stereochemistry of the complex or other subtle structural features is not likely to be important. Most members of this class are anionic.

The above requirements as well as others discussed in this article are satisfactorily met by $[Gd(DTPA)(H_2O)]^{2-}$ and $[Gd(DOTA)(H_2O)]^-$. Additional developments toward lowering toxicity even further may take place, but the more interesting challenge is to develop more specific agents as is discussed in the following sections.

The renal excretion of these agents yields the obvious application of imaging the kidneys, both for structural and functional information.[133,134] The status of blood flow to a tissue (perfusion) may be another application of these agents;[135,136] this requires the development of fast-imaging techniques to follow the rapid passage through the tissue.

The major use of these nonspecific agents is the detection of cerebral capillary breakdown or the enhancement of tissues with an increased extracellular volume. Both applications stem from the dependence of the bulk tissue $1/T_1$ on the volume of distribution of the paramagnetic agent. If we assume that water exchange between the extracellular and intracellular compartments is fast relative to their T_1's, then the bulk tissue $1/T_1$ before injection of the agent is given by eq 18, where f_{ex} is the fraction of water protons in the

$$(1/T_1)_{\text{pre inj}} = f_{ex}(1/T_1)_{ex,pre} + f_{in}(1/T_1)_{in} \quad (18)$$

extracellular space, $(1/T_1)_{ex,pre}$ is the extracellular relaxation rate in the absence of the paramagnetic species, and f_{in} is the intracellular fraction characterized by $(1/T_1)_{in}$. The extracellularly localized agent increases $(1/T_1)_{ex}$ directly, and the net change in the overall tissue $1/T_1$ is given by eq 19. If an agent equilibrates to

$$\Delta(1/T_1) = (1/T_1)_{\text{post inj}} - (1/T_1)_{\text{pre inj}}$$

$$= f_{ex}(1/T_1)_{ex,post} + f_{in}(1/T_1)_{in} - f_{ex}(1/T_1)_{ex,pre} - f_{in}(1/T_1)_{in}$$

$$= f_{ex}[(1/T_1)_{ex,post} - (1/T_1)_{ex,pre}] \quad (19)$$

roughly the same concentration in the extracellular space and, therefore, $(1/T_1)_{ex,post}$ is relatively constant in different tissues, then those tissues with the greatest fraction of extracellular space will yield the greatest NMR signal intensity changes. This has been observed for tumors and abscesses, which often exhibit increased interstitial volume.[4,7,134]

The most dramatic enhancement of lesions with these agents is seen in the brain (see Figure 11), where normal tissue exhibits little enhancement due to the impermeable nature of brain capillaries (the so-called blood–brain barrier) and the small intravascular volume of distribution (~5%) of the agent. The capillaries of tumors, however, do allow the passage of the complex into the interstitial space, allowing very selective enhancement.[7,22,134] The clinical trials of $[Gd(DTPA)(H_2O)]^{2-}$ in Europe and more recently in the United States have focused on brain lesions.[7]

B. Extracellular Distribution: Hepatobiliary Excretion

Hepatobiliary agents are the second most important class of potential NMR contrast agents. By virtue of

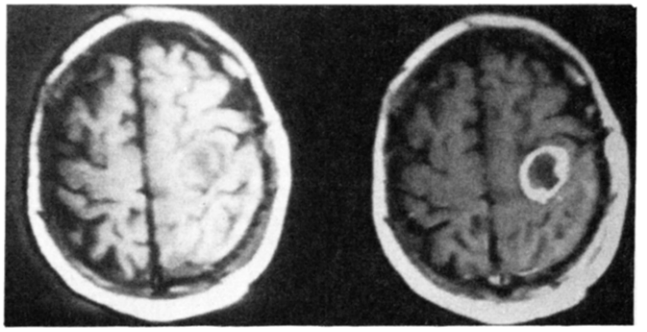

Figure 11. Transverse NMR images (0.6 T, 24 MHz) through the brain of a patient before (left) and 3 min after (right) intraveneous injection of $[Gd(DTPA)(H_2O)]^{2-}$ (dimeglumine salt; Schering/Berlex) at a dose of 0.1 mmol/kg. Characteristic ring enhancement of a tumor (high-grade astrocytoma) is seen in the postinjection image. Pulse sequence: spin echo, TR = 500, TE = 20 ms. (Courtesy of Dr. Thomas Brady, Massachusetts General Hospital.)

their efficient excretion from the body, the development of safe derivatives of this class seems likely. Additionally, in contrast to the nonspecific renal agents, hepatobiliary agents may give an indication of the status of specific cellular function: that of the hepatocytes of the liver.

The potential diagnostic utility of this class of NMR agents includes the following: (1) selective enhancement of normal, functioning liver tissue to aid in the detection of small lesions, such as metastatic tumors (focal liver disease); (2) indication of the status of liver function in order to detect diffuse liver disease such as cirrhosis; and (3) high-resolution visualization of bile ducts and the gallbladder.

Other forms of diagnostic hepatobiliary agents are radioactive ^{99m}Tc complexes[132,137] and iodinated CT agents.[138,139] Currently, various substituted ^{99m}Tc–phenylcarbamoylmethyliminodiacetic acid (^{99m}Tc–IDA) complexes are used in scintigraphic imaging to detect obstruction of bile ducts. However, the image resolu-

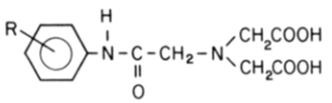

acetanilidoiminodiacetic acid

tion is very low compared with NMR, limiting biliary visualization. Also, the detection of small lesions in the liver by these complexes or other radiopharmaceuticals is not possible. The hepatobiliary agents for CT that have been evaluated are not used clinically due to their toxicity and high dose requirements.[139]

The mechanisms by which the hepatocytes of the liver extract certain molecules from the blood and secrete them into bile have not been refined.[131,140] Diagnostic hepatobiliary agents are generally anionic and are therefore thought to be taken up by the same carrier system that transports bilirubin IXα, the dicarboxylic acid breakdown product of heme, and various anionic dyes, such as bromosulfophthalein (BSP). Membrane proteins that are thought to play a crucial role in the uptake of these compounds have been identified, and it is likely that some type of carrier-mediated transport is at work. Separate anionic transport systems for fatty acids and bile acids apparently exist in addition to that for bilirubin. However, Berk and co-workers recently suggested that anionic compounds such as the ^{99m}Tc–IDA chelates may actually be taken up by more that one of the three carriers.[141] Alternatively, a single, complex system for all three types of anionic compounds may exist. An additional unsolved problem in hepatocellular uptake is how the molecules are extracted efficiently despite the tight binding by albumin in the blood that these molecules often exhibit. It is thought that some form of facilitated diffusion of the albumin–ligand complex may occur at or near the hepatocyte surface.

The structural and physicochemical properties required for hepatocellular uptake are poorly defined.[131] It is generally believed that high molecular weight (>300 for rats and >500 for humans) as well as the presence of both hydrophilic and lipophilic moieties will direct a compound to the bile in preference to the urine. The molecular weight requirement probably reflects the need for large lipophilic groups, especially aromatic rings, which may interact favorably with hydrophobic regions of the membrane receptor or other transport proteins. The ^{99m}Tc–IDA complexes, bilirubin, and various cholephilic dyes (such as BSP) possess at least two delocalized ring systems. The more polar moieties, especially ionized groups, are probably required for water solubility; molecules lacking these might precipitate in blood or become deposited in fat tissue or membranes. It is also likely that these groups, especially anionic residues, are important for electrostatic or hydrogen-bonding interactions at macromolecular binding sites.

Our group chose to evaluate $Fe(EHPG)^-$ as a prototype NMR hepatobiliary agent in view of these overall requirements and on the basis of early reports showing that EHPG induced the biliary excretion of Fe(III).[127,142] The complex contains coordinated carboxylates, two phenyl rings, net anionic charge, and octahedral coordination to the metal center.[143] These features are common to the suspected structures of the ^{99m}Tc–IDA agents as octahedral bis(IDA) complexes with a −1 charge.[132,137]

The fact that $Fe(EHPG)^-$ is coordinatively saturated and therefore relaxes water protons only via outer-sphere mechanisms did not dissuade us from evaluating it. The longitudinal relaxivity was found to be ~ 1 mM^{-1} s^{-1}, roughly four times less than $[Gd(DTPA)(H_2O)]^{2-}$, but nevertheless sufficient if the complex localizes in the liver and bile.[127]

The initial NMR imaging and biodistribution studies of $Fe(EHPG)^-$ were encouraging.[127] At a dose of 0.2 mmol/kg, the complex increases the $1/T_1$ of rat liver from approximately 3.2 to 4.3 s^{-1} (20 MHz, 37 °C) at 10 min postinjection, corresponding to ~ 1 mM concentration in the water space of the tissue. This localization yields a 200% increase in NMR image signal intensity on a 60-MHz system (Figure 12). (We demonstrated later that the degree of enhancement is dependent on the choice of pulse sequence parameters in accordance with theoretical expectations.[25]) The biliary clearance of the intact agent from the liver was noted for rats, rabbits, and dogs (see Figure 13).

The biliary excretion of ^{99m}Tc–IDA derivatives has been observed to be sensitive to simple chemical substitutions on the aromatic rings, stemming presumably

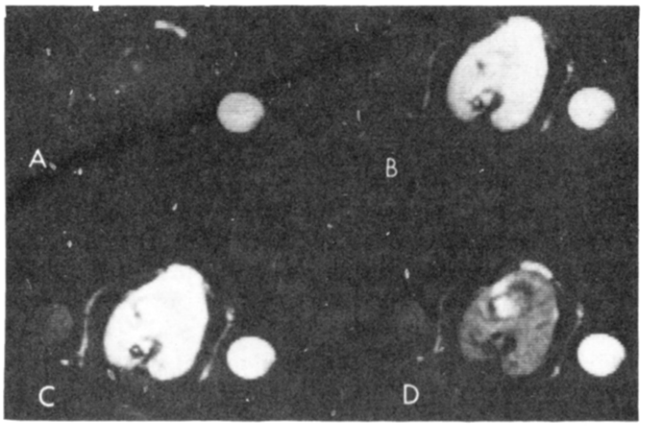

Figure 12. Transverse NMR images (1.4 T, 61.4 MHz) of the rat abdomen before (A) and 16, 56, and 182 min after (B–D, respectively) intraveneous injection of $Fe(EHPG)^-$ (0.2 mmol/kg). The selected slice is through the midportion of the liver. Two phantoms lie on either side of the animal. The liver signal intensity increases 200% in the first postinjection image due to the uptake of the complex by hepatocytes; clearance of the agent is noted over the 3-h imaging period. The pulse sequence utilized (inversion recovery TR = 1460, TI = 400, TE = 15 ms) emphasizes T_1 changes. Reprinted with permission from ref 127.

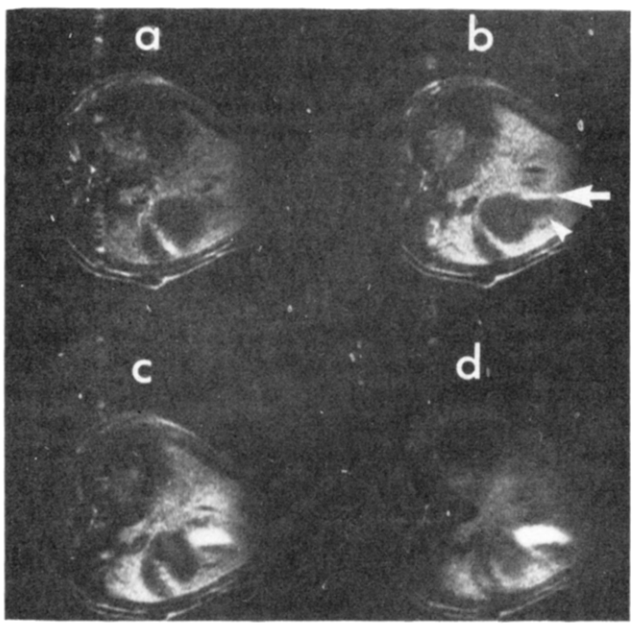

Figure 13. Transverse NMR images (0.6 T, 24 MHz) of the dog adbomen before (a) and 14, 50, and 60 min after (b–d, respectively) intraveneous injection of $Fe(EHPG)^-$ (0.2 mmol/kg). Enhancement of the liver and gallbladder is evident. Bile in the gallbladder prior to injection of the agent appears dark (arrowhead), whereas newly formed bile containing the paramagnetic agent appears bright (arrow) and layers on top. Reprinted with permission from ref 127.

from alterations in lipophilicity and binding affinity to albumin, receptor proteins, and/or cytosolic proteins.[144] Substituents in the para positions seem to be most effective, perhaps due to their penetration into hydrophobic binding sites.[145] Thus, in a recent study, we chose to compare $Fe(EHPG)^-$ with the 5-Me, 5-Cl, and 5-Br derivatives in order to explore the structural basis for biodistribution and imaging characteristics.[128] These particular para substituents were selected to study the effect of gradually increasing the lipophilicity of the complexes in the order H < Me < Cl < Br as predicted by additive π constants.[146] The three new derivatives exhibit higher degrees of lipophilicity (as

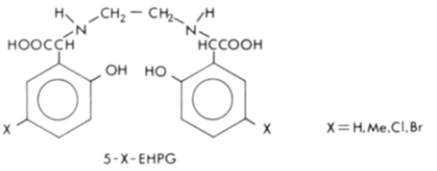

measured by octanol–buffer partition coefficients) and HSA binding affinity as well as varying degrees of improvement in liver-to-blood and bile-to-liver concentration ratios measured at 30 min postinjection. NMR imaging of the injected animals over 3-h periods revealed that the more lipophilic derivatives exhibit slower excretion from the liver.[128]

The sensitivity of the biodistribution behavior to changes in ring substituents is related to alterations in lipophilicity and/or protein- or receptor-binding affinity. Our results reveal a correlation between lipophilicity and albumin binding,[128] and one might expect similar behavior with binding to hepatocyte membrane receptors or cytosolic proteins. From the point of view of hepatobiliary agent design, the importance of these multiple binding events is that their net effect determines the pharmacokinetic rate constants that control relative tissue ratios. For example, a high affinity for serum albumin will decrease the rate of liver uptake, whereas strong binding to hepatocyte cytosol proteins will decrease the excretion rate. In the $Fe(5\text{-X-EHPG})^-$ series, liver/blood and intestine/liver ratios appeared optimal for the 5-Cl and 5-Me complexes with intermediate lipophilicity. Apparently, while some degree of lipophilicity (or protein-binding affinity) is necessary for liver uptake, complexes of higher lipophilicity exhibit slower kinetics most likely due to greater protein-binding affinity. This parabolic dependence of biological behavior with increasing lipophilicity has been well documented for other homologous series of molecules.[147] Its importance here is that it may be possible to tune the biodistribution properties of each new prototype hepatobiliary agent with appropriate substitutions.

We have begun to explore the structural basis of the binding interactions between heptobiliary-seeking complexes and proteins. HSA was chosen for initial studies for several reasons: (1) it possesses a remarkable capacity for binding structurally dissimilar anionic ligands;[148–151] (2) it modulates hepatobiliary excretion pharmacokinetics; (3) it represents an excellent target for intravascular contrast agents (see next section); and (4) it is an excellent model system of protein–chelate binding.

To examine the effects of subtle structural differences on HSA binding, we have isolated diastereomeric forms of $Fe(5\text{-Br-EHPG})^-$, a complex with relatively high binding affinity, and studied the binding using equilibrium dialysis. A preliminary account of this work has been published.[152] Structures of the racemic and meso diastereomers, based on the crystal structures of the unsubstituted isomers, are shown in Figure 14. The racemic enantiomers (*R*,*R* + *S*,*S*) are distorted octahedral complexes with two equivalent phenolates coordinated to the metal in the equatorial plane but twisted relative to one another; a twofold axis of symmetry bisects the N–Fe–N angle. The meso isomer (*R*,*S*), on the other hand, lacks this symmetry since one phenolate (from the (*S*)-carbon) coordinates to the iron

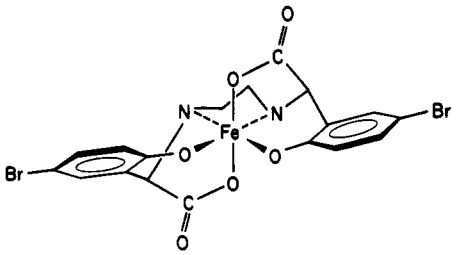

R,R-[Fe(5-Br-EHPG)$^-$]

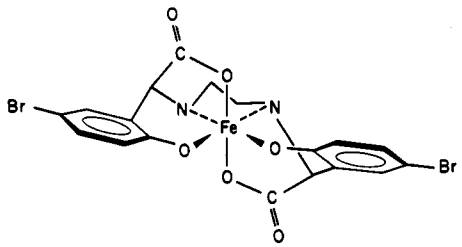

S,S-[Fe(5-Br-EHPG)$^-$]

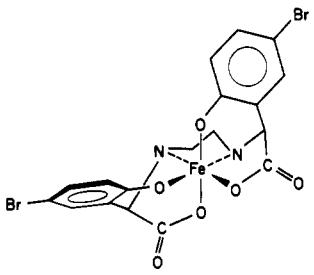

meso-[Fe(5-Br-EHPG)$^-$]

Figure 14. Structures of the Fe(5-Br-EHPG)$^-$ diastereomers. The two chiral centers on EHPG give rise to a set of racemic enantiomers (*R,R* + *S,S*) and the meso isomer (*R,S*).

at an axial site from above the equatorial plane.[143] The major difference between the diastereomers is the relative orientation of the two bromophenolate rings. Our binding studies to date consistently reveal that HSA possesses a higher affinity for the racemic isomer at low chelate/protein ratios. The stereoselectivity in the overall binding affinity indicates that molecular shape is an important component in these interactions in addition to the presumed hydrophobic, van der Waals, and electrostatic contributions.

Our understanding of these binding interactions is still at an early stage. The analysis of HSA–ligand binding isotherms in terms of the number of binding sites and their respective affinity constants can be difficult in the case when multiple, allosterically coupled sites exist. Likewise, the identification of common binding sites via displacement studies is often misleading. We have observed recently that the binding of both isomers of Fe(5-Br-EHPG)$^-$ is inhibited by chloride and thiocyanate; the much stronger displacement effect of the latter suggests competitive binding at one or more of the binding sites for the complexes. The specific regions of HSA exhibiting this generalized anion-binding behavior are not known.

A more interesting possible binding site for the complexes is the primary site for bilirubin IXα, the heme breakdown product excreted by the liver. Our initial binding studies,[152] performed in the presence of 0.15 M NaCl, showed that the remaining high-affinity binding

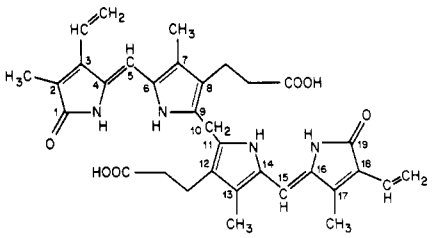

Bilirubin IXα

of *rac*-Fe(5-Br-EHPG)$^-$ to a single site on the protein was completely inhibited upon addition of 1 equiv of bilirubin IXα. *rac*-Fe(5-Br-EHPG)$^-$ shares certain chemical features in common with bilirubin IXα, such as anionic charge, hydrogen-bonding groups, and hydrophobic regions. In addition, a conformational analysis of bilirubin IXα reveals that the molecule can adopt an extended configuration that places its two dipyrromethene moieties in an orientation similar to that of the bromophenolate rings of *rac*-Fe(5-Br-EHPG)$^-$ (Figure 15). Thus, it is reasonable to propose that these two quite different molecules may share a common binding site on HSA. While more specific proof for the binding of this complex to the region on HSA containing the bilirubin IXα site is required, the structural comparison itself provides a link toward understanding the common in vivo chemistry and excretory behavior of bilirubin and various diagnostically useful metal chelates. The obvious inference is that the presence of two hydrophobic moieties on either side of a central anionic region may be important for binding not only to albumin but also to the hepatocyte membrane carrier protein.

C. Intravascular Distribution

A paramagnetic agent that would be confined in the intravascular space by molecular size or by binding to plasma proteins may have potential for the enhancement of normal, perfused tissues in preference to tissue with decreased blood supply. Additionally, these agents may be useful in enhancing smaller blood vessels by use of the novel NMR angiography techniques recently developed.[153]

An intravascular agent could be comprised of a paramagnetically labeled protein or polymer with a molecular weight greater than 60 000. Alternatively, a small molecular weight chelate could be designed to bind strongly to HSA. Both the noncovalent and covalent attachments would yield relaxivity enhancement.

HSA labeled heavily with multiple Gd–DTPA groups has been evaluated as an intravascular contrast agent.[154] The authors did not, however, address the possibility that Gd(III) may be released from such conjugates during proteolytic degradation (see section VC3).

The noncovalent approach seems more feasible. Our work on HSA–chelate interactions described above illustrates that the development of chelates that can bind to specific sites on HSA is possible. These chelates could be excreted harmlessly without metabolic degradation.

D. Tumor Localizing Agents

Two groups have described the use of synthetic paramagnetic metalloporphyrins to decrease the proton

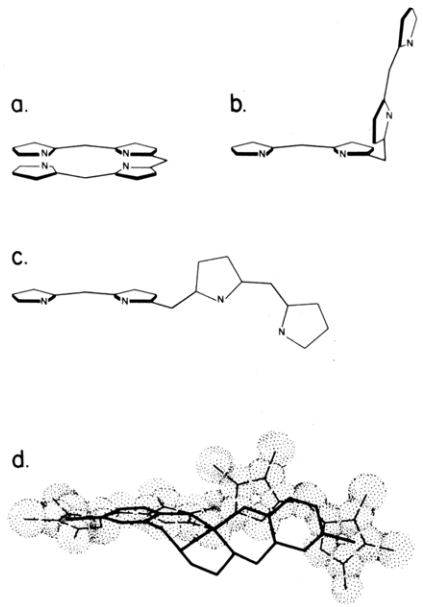

Figure 15. (a–c) possible conformations of bilirubin as a function of the two torsional angles about the central methylene: ϕ_1, N–C9–C10–C11; ϕ_2, N–C11–C10–C9. (a) $\phi_1 = \phi_2 = 0°$ (porphyrin-like configuration). (b) $\phi_1 = \phi_2 = -60.8°$ (intramolecular hydrogen-bonded form exhibited in the crystal structure of the dianion). (c) $\phi_1 = \phi_2 = -135°$ (example of an extended conformation). d. Superposition of a stick representation of (*R,R*)-Fe(5-Br-EHPG)$^-$ (thick lines) within the van der Waals surface of bilirubin (dots and dashed lines) in the extended conformation ($\phi_1 = \phi_2 = -135°$). The iron atom is placed at the central methylene of bilirubin, and the complex is positioned to illustrate the similarity between the orientation of its bromophenolate rings with respect to the dipyrromethene moieties of bilirubin. In a–d, selected peripheral atoms and all hydrogens have been omitted for clarity. In d, the two carboxylates of the complex are not displayed. Reprinted with permission from ref 152. Copyright 1987 American Chemical Society.

relaxation times of tumors.[120,155] The properties of these complexes are somewhat different compared with the free porphyrin–ligand mixture, known as hematoporphyrin derivative, which localizes in tumors and is used in phototherapy.[156] Nevertheless, some degree of retention of synthetic complexes, such as Mn^{III}(TPPS), in tumors has been observed. The mechanism for this retention is not known, and this obviates a rational approach to the design of these agents. However, the stability and high relaxivity of these complexes in addition to their unexplained tumor localization do make them attractive prototype contrast agents.

An alternative approach to tumor imaging involves the use of labeled monoclonal antibodies specific to a particular tumor line. Though greeted initially with enthusiasm, this method is likely to be useful only in radioimaging, where only miniscule concentrations of the label are needed. For NMR imaging, the required concentration of paramagnetic species is roughly 10–100 μM, whereas the concentration of antigenic sites in tumors is 0.1 μM or less (for example, see ref 157). Even if these sites could be saturated with paramagnetically labeled antibody molecules, such conjugates would require 100–1000 chelates/molecule for significant relaxation time differences. Coupled with the obvious problems of the potential toxicity and lower antigenic affinity of these conjugates, this approach is not likely to be clinically feasible. Perhaps other diagnostically useful target sites of higher concentration exist for "magneto–immunoimaging".

VIII. Concluding Remarks

The development of metal complexes as NMR imaging agents embraces a wide range of disciplines from radiology to chemical physics. In between these extremes, a number of important problems exist for chemists with NMR, bioinorganic, or coordination chemistry interests. These include the quantitative understanding of relaxivity, the design of stable chelating agents, and the structural basis for chelate–macromolecule interactions. Basic research in these and related areas will also contribute to other areas of chemistry.

In comparing the development of NMR agents with that of inorganic radiopharmaceuticals, it is apparent that the former will require a great deal more characterization due to the complexities inherent in NMR relaxation phenomena and the higher dose requirements. Though the approval of NMR agents for human use may be more difficult to obtain, the promise of routine patient screening with high-resolution, contrast-enhanced NMR imaging will certainly catalyze the development of safe agents. It is likely, therefore, that these "magnetopharmaceuticals" will play an important role in the extension of NMR into diagnostic medicine.

Note Added in Proof. A different mechanism for NMR contrast enhancement with paramagnetic metal chelates has been recently demonstrated by the Massachusetts General Hospital Group. If present in relatively high concentrations, paramagnetic complexes can significantly increase the bulk magnetic susceptibility of a given tissue compartment. We believe that when an agent is not homogeneously distributed throughout the tissue, microscopic magnetic field gradients can be induced. The diffusion of nuclei through such gradients causes efficient transverse relaxation (known as a T_2* contribution) and signal diminution. Early studies showed that injection of Dy(DTPA)$^{2-}$ (Dy(III) has a magnetic moment of 10 Bohr magnetons) causes a very transient signal decrease in liver signal intensity on spin echo NMR images (Lauffer, R. B.; Saini, S.; Brady, T. J., unpublished results). Further work using different lanthanide DTPA chelates confirmed the effect on brain signal intensity and showed that the degree of signal loss correlated with the magnetic moment of the metal ion (Villringer, A. et al., 5th Annual Meeting of the Society of Magnetic Resonance in Medicine, Montreal, 1986; Villringer, A. et al., *Magn. Reson. Med.*, in press). It is thought that this method will be especially useful in examining cardiac and brain perfusion, particularly when combined with the recently developed fast imaging techniques (gradient echo or echo planar).

IX. Addendum: Abbreviations

ATP	adenosine 5′-triphosphate
bpy	2,2′-bipyridine
BSP	bromosulfophthalein
CDTA	*trans*-1,2-cyclohexylenedinitrilotetraacetic acid
dien	diethylenetriamine
dipic	dipicolinate, or 2,6-dicarboxypyridine

DOTA	1,4,7,10-tetraazacyclododecane-*N*,*N*′,*N*″,*N*‴-tetraacetic acid
DTPA	diethylenetriaminepentaacetic acid
EDDA	ethylenediaminediacetic acid
EDTA	ethylenediaminetetraacetic acid
EGTA	ethylene glycol(2-aminoethyl ether)tetraacetic acid
EHPG	*N*,*N*′-ethylenebis(2-hydroxyphenylglycine)
en	ethylenediamine
HBED	*N*,*N*′-bis(2-hydroxybenzyl)ethylenediaminediacetic acid
HEDTA	hydroxyethylethylenediaminetriacetic acid
HSA	human serum albumin
IDA	phenylcarbamoylmethyliminodiacetic acid
NMRD	nuclear magnetic relaxation dispersion, or the magnetic field dependence of relaxivity
NOTA	1,4,7-triazacyclononane-*N*,*N*′,*N*″-triacetic acid
NTA	nitrilotriacetic acid
PDTA	1,3-propylenediaminetetraacetic acid
phen	1,10-phenanthroline
PRE	proton relaxation enhancement, or the enhancement in relaxivity that occurs when the rotational correlation time of a paramagnetic species is increased
terpy	2,2′,2″-terpyridine
TETA	1,4,8,11-tetraazacyclotetradecane-*N*,*N*′,*N*″,*N*‴-tetraacetic acid
tetren	tetraethylenepentamine
TPPS	tetrakis(4-sulfonatophenyl)porphyrin
TMPyP	tetrakis(*N*-methyl-4-pyridyl)porphyrin
trien	triethylenetetraamine
TTHA	triethylenetetraaminehexaacetic acid
ZFS	zero-field splitting
[12]aneN$_4$	cyclen, or 1,4,7,10-tetraazacyclododecane
[14]aneN$_4$	cyclam, or 1,4,8,11-tetraazacyclotetradecane
q	number of primary coordination sphere water molecules
q'	number of second coordination sphere water molecules
r	distance between nucleus and unpaired electron spin density
R_1	longitudinal relaxivity
τ_c	overall correlation time for dipolar relaxation
τ_D	translational diffusion correlation time
τ_e	overall correlation time for contact relaxation
τ_M	residence time of primary coordination sphere water molecules
τ_M'	residence time of second coordination sphere water molecules
τ_R	rotational correlation time
τ_{S0}	T_{1e} at zero field
τ_V	correlation time modulating electron spin relaxation
T_1	longitudinal (or spin–lattice) nuclear relaxation time
T_2	transverse (or spin–spin) nuclear relaxation time
T_{1e}	longitudinal electron spin relaxation time

Acknowledgments. This work was supported by PHS Grants CA42430 and GM37777 awarded by the National Cancer Institute and the National Institute of General Medical Sciences, DHHS, respectively. I thank Dr. Serge Conti for designing the computer programs for NMRD simulations and Dr. Seymour Koenig for preprints of accepted manuscripts as well as helpful discussions.

Registry No. Water, 7732-18-5.

X. References

(1) Koutcher, J. A.; Burt, C. T.; Lauffer, R. B.; Brady, T. J. *J. Nucl. Med.* **1984**, *25*, 506.
(2) Mendonca-Dias, M. A.; Gaggelli, E.; Lauterbur, P. *Semin. Nucl. Med.* **1983**, *12*, 364.
(3) Brasch, R. C. *Radiology (Easton, Pa.)* **1983**, *147*, 781.
(4) Wolf, G. L.; Burnett, K. R.; Goldstein, E. J.; Joseph, P. M. In *Magnetic Resonance Annual 1985*; Kressel, H., Ed.; Raven: New York, 1985; p 231.
(5) Engelstad, B. L.; Brasch, R. C. In *Biomedical Magnetic Resonance*; James, T. L., Margulis, A. R., Eds.; Radiology Research and Education Foundation: San Francisco, 1984; p 139.
(6) Runge, V. M., Claussen, C., Felix, R., James, A. E., Jr., Eds. In *Contrast Agents in Magnetic Resonance Imaging*; Excerpta Medica: Princeton, NJ, 1986.
(7) Tweedle, M. F.; Brittain, H. G.; Eckelman, W. C. In *Magnetic Resonance Imaging*, 2nd ed.; Partain, C. L., et al., Eds.; W. B. Saunders: Philadelphia, 1987, in press.
(8) Bloch, F.; Hansen, W. W.; Packard, M. *Phys. Rev.* **1948**, *70*, 474.
(9) (a) Bloembergen, N.; Purcell, E. M.; Pound, R. V. *Phys. Rev.* **1948**, *73*, 678. (b) Bloembergen, N. *J. Chem. Phys.* **1957**, *27*, 572.
(10) Kubo, R.; Tomita, K. *J. Phys. Soc. Jpn.* **1954**, *9*, 888.
(11) Solomon, I. *Phys. Rev.* **1955**, *99*, 559.
(12) Eisinger, J.; Shulman, R. G.; Blumberg, W. E. *Nature (London), New Biol.* **1961**, *192*, 963.
(13) Dwek, R. A. In *Nuclear Magnetic Resonance in Biochemistry, Applications to Enzyme Systems*; Clarendon: Oxford, 1973; Chapters 9–11.
(14) Mildvan, A. S. *Annu. Rev. Biochem.* **1974**, *43*, 357.
(15) Burton, D. R.; Forsen, S.; Karlstrom, G.; Dwek, R. A. *Prog. Nucl. Magn. Reson. Spectrosc.* **1979**, *13*, 1.
(16) Lauterbur, P. C. *Nature (London), New Biol.* **1973**, *242*, 190.
(17) (a) Hinshaw, W. S.; Bottomley, P. A.; Holland, G. N. *Nature (London)* **1977**, *270*, 722. (b) Andrew, E. R.; Bottomley, P. A.; Hinshaw, W. S.; et al. *Phys. Med. Biol.* **1977**, *22*, 971. (c) Damadian, R.; Goldsmith, M.; Minkoff, L. *Physiol. Chem. Phys.* **1977**, *9*, 97.
(18) Lauterbur, P. C.; Mendoca-Dias, M. H.; Rudin, A. M. In *Frontier of Biological Energetics*; Dutton, P. L.; Leigh, L. S., Scarpa, A., Eds.; Academic: New York, 1978; p 752.
(19) Brady, T. J.; Goldman, M. R.; Pykett, I. L.; et al. *Radiology (Easton, Pa.)* **1982**, *144*, 343.
(20) Goldman, M. R.; Brady, T. J.; Pykett, I. L.; et al. *Circulation* **1982**, *66*, 1012.
(21) Young, I. R.; Clarke, G. J.; Gailes, D. R.; et al. *Comput. Tomogr.* **1981**, 5, 534.
(22) Carr, D. H.; Brown, J.; Bydder, G. M.; et al. *Lancet* **1984**, *1*, 484.
(23) (a) Pykett, I. L. *Sci. Am.* **1982**, *246*, 78. (b) Pykett, I. L.; Newhouse, J. H.; Buonanno, F. S.; et al., *Radiology (Easton, Pa.)* **1982**, *143*, 157. (c) Mansfield, P.; Morris, P. G. In *NMR Imaging in Biomedicine*; Academic: New York, 1982. (d) Kaufman, L.; Crooks, L. E.; Margulis, A. R., Eds. In *Nuclear Magnetic Resonance Imaging in Medicine*; Igaku-Shoin: New York, 1981.
(24) Farrar, T. C.; Becker, E. D. *Pulse and Fourier Transform NMR*; Academic: New York, 1971.
(25) Greif, W. L.; Buxton, R. B.; Lauffer, R. B.; et al. *Radiology* **1985**, *157*, 461.
(26) La Mar, G. N., Horrocks, W. D., Holm, R. G., Eds. *NMR of Paramagnetic Molecules*; Academic: New York, 1973.
(27) Koenig, S. H. *J. Magn. Reson.* **1978**, *31*, 1.
(28) Koenig, S. H.; Brown, R. D. III *Magn. Reson. Med.* **1984**, *1*, 478.
(29) Koenig, S. H.; Brown, R. D. III *J. Magn. Reson.* **1985**, *61*, 426.
(30) Bertini, I.; Luchinat, C. In *NMR of Paramagnetic Molecules in Biological Systems*; Benjamin/Cummings: Menlo Park, CA, 1986.
(31) Kowalewski, J.; Nordenskiold, L.; Benetis, N.; Westlund, P.-O. *Prog. Nucl. Magn. Reson. Spectrosc.* **1985**, *17*, 141.
(32) Bloembergen, N.; Morgan, L. O. *J. Chem. Phys.* **1961**, *34*, 842.
(33) Friedman, H. L. In *Protons and Ions Involved in Fast Dynamic Phenomena*; Laszlo, P., Ed.; Elsevier: Amsterdam, 1978; pp 27–42.

(34) Koenig, S. H.; Brown, R. D.; Studebaker, J. *Cold Spring Harbor Symp. Quant. Biol.* **1971**, *36*, 551.
(35) Bertini, I.; Luchinat, C.; Kowaleski, J. *J. Magn. Reson.* **1985**, *62*, 235.
(36) Bertini, I.; Luchinat, C.; Mancini, M.; Spina, G. *J. Magn. Reson.* **1984**, *59*, 213.
(37) Banci, L.; Bertini, I.; Briganti, F.; Luchinat, C. *J. Magn. Reson.* **1986**, *66*, 58.
(38) Redfield, A. G. *Adv. Magn. Reson.* **1965**, *1*, 1.
(39) Lindner, U. *Ann. Phys. (Leipzig)* **1965**, *16*, 319.
(40) Friedman, H. L.; Holz, M.; Hertz, H. G. *J. Chem. Phys.* **1979**, *70*, 3369.
(41) (a) Benetis, N.; Kowalewski, J.; Nordenskiold, L.; Wennerstrom, H.; Westlund, P.-O. *Mol. Phys.* **1983**, *48*, 329. (b) Benetis, N.; Kowalewski, J.; Nordenskiold, L.; Wennerstrom, H.; Westlund, P.-O. *Mol. Phys.* **1983**, *50*, 515. (c) Benetis, N.; Kowlewski, J.; Nordenskiold, L.; Wennerstrom, H.; Westlund, P.-O. *J. Magn. Reson.* **1984**, *58*, 261. (d) Westlund, P.-O.; Wennerstrom, H.; Nordenskiold, L.; Kowalewski, J.; Benetis, N. *J. Magn. Reson.* **1984**, *59*, 91. (e) Benetis, N.; Kowalewski, J.; Nordenskiold, L.; Edlund, U. *J. Magn. Reson.* **1984**, *58*, 282.
(42) Kushnir, T.; Navon, G. *J. Magn. Reson.* **1984**, *56*, 373.
(43) (a) Gueron, M. *J. Magn. Reson.* **1975**, *19*, 58. (b) Vega, A. J.; Fiat, D. *Mol. Phys.* **1976**, *31*, 347.
(44) (a) Pfeifer, H. *Ann. Phys. (Leipzig)* **1961**, *8*, 1. (b) Pfeifer, H. *Z. Naturforsch. A: Astrophys., Phys. Phys. Chem.* **1962**, *17*, 279. (c) Pfeifer, H. *Biochim. Biophys. Acta* **1963**, *66*, 434.
(45) Hubbard, P. S. *Proc R. Soc. London, A.* 1966, *291*, 537.
(46) (a) Hwang, L. P.; Freed, J. H. *J. Chem. Phys.* **1975**, *63*, 4017. (b) Freed, J. H. *J. Chem. Phys.* **1978**, *68*, 4034.
(47) Ayant, Y.; Belorizky, E.; Alizon, J.; Gallice, J. *J. Chem. Phys.* **1975**, *36*, 991.
(48) Hausser, R.; Noack, F. *Z. Naturforsch. A: Astrophys. Phys. Phys. Chem.* **1965**, *20*, 1668.
(49) Koenig, S. H.; Brown, R. D.; Lindstrom, T. R. *Biophys. J.* **1981**, *34*, 397.
(50) Koenig, S. H.; Brown, R. D. *Ann. N.Y. Acad. Sci.* **1973**, *222*, 752.
(51) (a) Borah, B.; Bryant, R. G. *J. Chem. Phys.* **1981**, *75*, 3297. (b) Polnaszek, C. F.; Bryant, R. G. *J. Am. Chem. Soc.* **1984**, *106*, 429. (c) Polnaszek, C. F.; Bryant, R. G. *J. Chem. Phys.* **1984**, *81*, 4038.
(52) Bennett, H. F.; Brown, R. D.; Koenig, S. H.; Swartz, H. M. *Magn. Res. Med.* **1987**, *4*, 93.
(53) Nientiedt, H.-W.; Bundfuss, K.; Muller-Warmuth, W. *J. Magn. Reson.* **1981**, *43*, 154.
(54) Hunt, J. P.; Friedman, H. L. In Progress in Inorganic Chemistry; Lippard, S. J., Ed.; Wiley: New York, 1983; Vol. 30, 359.
(55) Marcus, Y. In *Ion Solvation*; Wiley: Chichester, U.K., 1985; Chapter 5.
(56) Waysbort, D.; Navon, G. *J. Phys. Chem.* **1980**, *84*, 674.
(57) Amis, E. S.; Hinton, J. F. In *Solvent Effects on Chemical Phenomena*; Academic: New York, 1973; Vol. 1.
(58) Davis, T. S.; Fackler, J. P. *Inorg. Chem.* **1966**, *5*, 242.
(59) Frankel, L. S. *J. Phys. Chem.* **1969**, *73*, 3897.
(60) Frankel, L. S. *J. Phys. Chem.* **1970**, *74*, 1645.
(61) Langford, C. H.; White, J. F. *Can. J. Chem.* **1967**, *45*, 3049.
(62) Behrendt, S.; Langford, C. H.; Frankel, L. S. *J. Am. Chem. Soc.* **1969**, *91*, 2236.
(63) Chan, S. O.; Eaton, D. R. *Can. J. Chem.* **1976**, *54*, 1332.
(64) Nekipelov, V. M.; Zamaraev, K. I. *Coord. Chem. Rev.* **1985**, *61*, 185.
(65) Kim, M. B.; Makinen, M. W. *J. Magn. Reson.* **1986**, *70*, 89.
(66) Luz, Z.; Meiboom, S. *J. Chem. Phys.* **1964**, *40*, 2686.
(67) McCandlish, E. F. K.; Michael, T. K.; Neal, J. A.; Langafelter, E. C.; Rose, N. J. *Inorg. Chem.* **1978**, *17*, 1384.
(68) Bertini, I.; Briganti, F.; Koenig, S. H.; Luchinat, C. *Biochemistry* **1985**, *24*, 6287.
(69) Koenig, S. H.; Brown, R. D. III In *Magnetic Resonance Annual 1987*; Kressel, H. Y., Ed.; Raven: New York, 1987; in press.
(70) Koenig, S. H.; Baglin, C.; Brown, R. D. III; Brewer, C. F. *Magn. Reson. Med.* **1984**, *1*, 496.
(71) Koenig, S. H.; Baglin, C.; Brown, R. D. III *Magn. Reson. Med.* **1985**, *2*, 283.
(72) Geraldes, C. F. G. C.; Sherry, A. D.; Brown, R. D. III; Koenig, S. H. *Magn. Reson. Med.* **1986**, *3*, 242.
(73) Koenig, S. H.; Brown, S. H.; Spiller, M. *Magn. Reson. Med.* **1987**, *4*, 252.
(74) Oakes, J.; Smith, E. G. *J. Chem. Soc., Faraday Trans. 2* **1981**, *77*, 299.
(75) Bloch, J.; Navon, G. *J. Inorg. Nucl. Chem.* **1980**, *42*, 693.
(76) Oakes, J.; van Kralingen, C. G. *J. Chem. Soc., Dalton Trans.* **1984**, 1133.
(77) Alsaadi, B. M.; Rossotti, F. J. C.; Williams, R. J. P. *J. Chem. Soc., Dalton Trans.* **1980**, 813.
(78) Alsaadi, B. M.; Rossotti, F. J. C.; Williams, R. J. P. *J. Chem. Soc., Dalton Trans.* **1980**, 2151.
(79) Stezowski, J. J.; Hoard, J. L. *Isr. J. Chem.* **1984**, *24*, 323.
(80) Spirlet, M. R.; Rebizant, J.; Dexreux, J. F.; Loncin, F. *Inorg. Chem.* **1984**, *23*, 359.
(81) Spirlet, M. R.; Rebizant, J.; Loncin, F.; Dexreux, J. F. *Inorg. Chem.* **1984**, *23*, 4278.
(82) Bryden, C. C.; Reilley, C. N. *Anal. Chem.* **1982**, *54*, 610.
(83) Geier, G.; Karlen, V.; Zelewsky, A. G. *Helv. Chim. Acta* **1969**, *52*, 1967.
(84) Hoard, J. L.; Lee, B.; Lind, M. D. *J. Am. Chem. Soc.* **1965**, *87*, 1612.
(85) Oakes, J.; Smith, E. G. *J. Chem. Soc., Faraday Trans. 1* **1983**, *79*, 543.
(86) Koenig, S. H.; Brown, R. D. III In *The Coordination Chemistry of Metalloenzymes*; Bertini, I., Drago, R. S., Luchinat, C., Eds.; Reidel: Dordrecht, 1983; p 19.
(87) Lauffer, R. B.; Brady, T. J. *Magn. Reson. Imaging* **1985**, *3*, 11.
(88) Lauffer, R. B.; Brady, T. J.; Brown, R. D.; Baglin, C.; Koenig, S. H. *Magn. Reson. Med.* **1986**, *3*, 541.
(89) Tweedle, M. F.; Gaughan, G. T.; Hagan, J.; Wedeking, P. W. *Int. J. Nucl. Med. Biol.*, in press.
(90) Brading, A. F.; Jones, A. W. *J. Physiol. (London)* **1969**, *200*, 387.
(91) Koenig, S. H.; Spiller, M.; Brown, R. D. III; Wolf, G. L. *Magn. Reson. Med.* **1986**, *3*, 791.
(92) Spiller, M.; Koenig, S. H.; Wolf, G. L.; Brown, R. D. III Presented at the 4th Annual Meeting of the Society of Magnetic Resonance in Medicine, London, 1985.
(93) (a) Kang, Y. S.; Gore, J. C. *Invest. Radiol.* **1984**, *19*, 399. (b) Kang, Y. S.; Gore, J. C.; Armitage, I. M. *Magn. Reson. Med.* **1984**, *1*, 396.
(94) Koenig, S. H.; Brown, R. D. III; Goldstein, E. J.; Burnett, K. R.; Wolf, G. L. *Magn. Reson. Med.* **1985**, *2*, 159.
(95) Waysbort, D.; Navon, G. *J. Chem. Phys.* **1978**, *68*, 3074.
(96) Ferraris, G.; Franchini-Angela, M. *Acta Crystallogr. Sect. B: Struct. Crystallogr. Cryst. Chem.* **1972**, *B28*, 3572.
(97) Narten, A. H.; Hahn, R. L. *Science (Washington, D.C.)* **1982**, *217*, 1249.
(98) Kennedy, S. D.; Bryant, R. G. *Magn. Reson. Med.* **1985**, *2*, 14.
(99) Banci, L.; Bertini, I.; Luchinat, C. *Inorg. Chim. Acta* **1985**, *100*, 173.
(100) James, T. L. In *Nuclear Magnetic Resonance in Biochemistry*; Academic: New York, 1975; p 39.
(101) (a) Sachs, F. In *Magnetic Resonance in Colloid and Interface Science*; Resing, H. A., Wade, C. G., Eds.; American Chemical Society: Washington, DC, 1976; p 504. (b) Sachs, F.; Latorre, R. *Biophys. J.* **1974**, *14*, 316. (c) Morse, P. D. II; Lusczakoski, D. M.; Simpson, D. A. *Biochemistry* **1979**, *18*, 5021. (d) Hendrick, W. R.; Mathew, A.; Zimbrick, J. D.; Whaley, T. W. *J. Magn. Reson.* **1979**, *36*, 207. (e) Mastro, A. M.; Babich, M. A.; Taylor, W. D.; Keith, A. D. *Proc. Natl. Acad. Sci. U.S.A.* **1984**, *81*, 3414.
(102) Woessner, D. *J. Chem. Phys.* **1962**, *36*, 1.
(103) (a) Karplus, M.; McCammon, J. A. *CRC Crit. Rev. Biochem.* **1981**, *9*, 293. (b) Karplus, M. *Adv. Biophys.* **1984**, *18*, 165.
(104) Jardetsky, O.; Roberts, G. C. K. In *NMR in Molecular Biology*; Academic: Orlando, FL, 1981; Chapter 12.
(105) Likhtenshtein, G. I. *Spin Labelling Methods in Molecular Biology*; Wiley: New York, 1976; Chapter 7.
(106) Lauffer, R. B.; Betteridge, D. R.; Padmanabhan, S.; Brady, T. J. Presented at the 4th Annual Meeting of the Society of Magnetic Resonance in Medicine, London, 1985.
(107) Lauffer, R. B.; Betteridge, D. R.; Padmanabhan, S.; Brady, T. J. *Int. J. Nucl. Med. Biol.*, in press.
(108) La Mar, G. N.; Walker, F. A. *J. Am. Chem. Soc.* **1973**, *95*, 6950.
(109) Swift, T. J.; Connick, R. E. *J. Chem. Phys.* **1962**, *37*, 307.
(110) Hunt, J. P. *Coord. Chem. Rev.* **1971**, *7*, 1.
(111) Zetter, M. S.; Grant, M. W.; Wood, E. J.; Dodgen, H. W.; Hunt, J. P. *Inorg. Chem.* **1972**, *11*, 2701.
(112) Rablen, D. P.; Dodgen, H. W.; Hunt, J. P. *Inorg. Chem.* **1976**, *15*, 931.
(113) Coates, J. H.; Hadi, D. A.; Lincoln, S. F.; Dodgen, H. W.; Hunt, J. P. *Inorg. Chem.* **1981**, *20*, 707.
(114) Margerum, D. W.; Cayley, G. R.; Weatherburn, D. C.; Pagenkopf, G. K. In *Coordination Chemistry*; Martell, A. E., Ed.; American Chemical Society: Washington, DC, 1978; Vol. 2, Chapter 1.
(115) Ostrich, I. J.; Liu, G.; Dodgen, H. W.; Hunt, J. P. *Inorg. Chem.* **1980**, *19*, 619.
(116) Southwood-Jones, R. V.; Earl, W. L.; Newman, K. E.; Merbach, A. E. *J. Chem. Phys.* **1980**, *73*, 5909.
(117) Sinha, S. P. *Struct. and Bonding (Berlin)* **1976**, *25*, 69.
(118) Weinmann, H.-J.; Brasch, R. C.; Press, R. C.; Wesbey, G. E. *AJR, Am. J. Roentgenol.* **1984**, *142*, 619.
(119) Luckey, T. D.; Venugopal, B. In *Metal Toxicity in Mammals*; Plenum: New York, 1977; Vol. 1.
(120) Lyon, R. C.; Faustino, P. J.; Cohen, J. S.; Katz, A.; Mornex, F.; Colcher, D.; Baglin, C.; Koenig, S. H.; Hambright, P. *Magn. Reson. Med.* **1987**, *4*, 24.

(121) Martell, A. E. In *Development of Iron Chelates for Clinical Use*; Martell, A. E., Anderson, W. F., Badman, D. G., Eds.; Elsevier North Holland: New York, 1981; p 67.
(122) Moerlein, S. M.; Welch, M. J. *Int. J. Nucl. Med. Biol.* **1981**, *8*, 277.
(123) Raymond, K. N.; Pecoraro, V. L.; Weitl, F. L. In *Development of Iron Chelates for Clinical Use*; Martell, A. E., Anderson, W. F., Badman, D. G., Eds.; Elsevier North Holland: New York, 1981; p 165.
(124) Desreux, J. F.; Barthelemy, P. P. *Int. J. Nucl. Med. Biol.*, in press.
(125) Magerstadt, M.; Gansow, O. A.; Brechbiel, M. W.; et al. *Magn. Reson. Med.* **1986**, *3*, 808.
(126) Yeh, S. M.; Meares, C. F.; Goodwin, D. A. *J. Radioanal. Nucl. Chem.* **1979**, *53*, 327.
(127) Lauffer, R. B.; Greif, W. L.; Stark, D. D.; Vincent, A. C.; Saini, S.; Wedeen, V. J.; Brady, T. J. *J. Comput. Assist. Tomogr.* **1985**, *9*, 431.
(128) Lauffer, R. B.; Vincent, A. C.; Padmanabhan, S.; Villringer, A.; Saini, S.; Elmaleh, D. R.; Brady, T. J. *Magn. Reson. Med.* **1987**, *4*, 582.
(129) Jackels, S. C.; Kroos, B. R.; Hinson, W. H.; Karstaedt, N.; Moran, P. R. *Radiology (Easton, Pa.)* **1986**, *159*, 525.
(130) Venkatachalam, M. A.; Rennke, H. G. *Circ. Res.* **1978**, *43*, 337.
(131) Klaassen, C. D.; Watkins, J. B. III *Pharmacol. Rev.* **1984**, *36*, 1.
(132) Heindel, N. D.; Burns, H. D.; Honda, T.; Brady, L. W. In *The Chemistry of Radiopharmaceuticals*; Masson: New York, 1978.
(133) Wolf, G. L.; Fobben, E. S. *Invest. Radiol.* **1984**, *19*, 324.
(134) Brasch, R. C.; Weinmann, H.-J.; Wesbey, G. E. *AJR, Am. J. Roentgenol.* **1984**, *142*, 625.
(135) McNamara, M. T.; Tscholakoff, D.; Revel, D.; et al. *Radiology (Easton, Pa.)* **1986**, *158*, 765.
(136) Liu, P.; Villringer, A.; Lauffer, R. B.; et al. *Radiology (Easton, Pa.)*, in press.
(137) Chervu, L. R.; Nunn, A. D.; Loberg, M. D. *Semin. Nucl. Med.* **1984**, *12*, 5.
(138) Koehler, R. E.; Stanley, R. J.; Evans, R. G. *Radiology (Easton, Pa.)* **1979**, *132*, 115.
(139) Moss, A. A. In *Computed Tomography of the Body*; Moss, A. A., Gamsu, G., Genant, H. K., Es.; Saunders: Philadelphia, 1983; p 615.
(140) Berk, P. D.; Stremmel, W. In *Progress in Liver Disease*; Popper, H., Schaffner, F., Eds.; Grune & Stratton: Orlando, FL, 1985; Vol. VIII, pp 125–144.
(141) Okuda, H.; Nunes, R.; Vallabhajosula, S.; Strahun, A.; Goldsmith, S. J.; Berk, P. D. *J. Hepatol.* **1986**, *3*, 251.
(142) Haddock, E. P.; Zapolski, E. J.; Rubin, M. *Proc. Soc. Exp. Biol. Med.* **1965**, *120*, 663.
(143) Bailey, N. A.; Cummins, D.; McKenzie, E. D.; Worthington, J. M. *Inorg. Chim. Acta* **1981**, *50*, 111.
(144) Nunn, A. D.; Loberg, M. D.; Conley, R. A. *J. Nucl. Med.* **1983**, *24*, 423.
(145) Nunn, A. D. *J. Labelled Compd. Radiopharm.* **1981**, *18*, 155.
(146) Hansch, C.; Leo, A. In *Substituent Constants for Correlation Analysis in Chemistry and Biology*; Wiley: New York, 1979.
(147) Kubinyi, H. *Arzneim.-Forsch.* **1979**, *29*, 1067.
(148) Kragh-Hansen, U. *Pharmacol. Rev.* **1981**, *33*, 17–53.
(149) Fehske, K. J.; Muller, W. E.; Wollert, U. *Biochem. Pharmacol.* **1981**, *30*, 681–692.
(150) Brown, J. R.; Shockley, P. In *Lipid-Protein Interactions*; Jost, P., Griffith, O. H., Eds.; Wiley: New York, 1982; pp 25–68.
(151) Peters, T., Jr. *Adv. Protein Chem.* **1985**, *37*, 161–245.
(152) Lauffer, R. B.; Vincent, A. C.; Padmanabhan, S.; Meade, T. J. *J. Am. Chem. Soc.* **1987**, *109*, 2216.
(153) Wedeen, V. J.; Meuli, R. A.; Edelman, R. R.; et al. *Science (Washington, D.C.)* **1985**, *230*, 946.
(154) Schmeidl, U.; Ogan, M.; Paajanen, H.; et al. *Radiology (Easton, Pa.)* **1987**, *162*, 205.
(155) Fiel, R. J.; Button, T. M.; Gilani, S., et al. *Magn. Reson. Imaging* **1987**, *5*, 149.
(156) Doiron, D. R.; Gomer, C. J., Eds. *Porphyrin Localization and Treatment of Tumors*; Liss: New York, 1984.
(157) Unger, E. C.; Totty, W. G.; Neufeld, D. M., et al. *Invest. Radiol.* **1985**, *20*, 693.